

NASA CONTRACTOR REPORT

**N 73 22089**  
NASA CR-62086

# **GEOS-II C-BAND RADAR SYSTEM PROJECT**

## **FINAL REPORT**

### **MARINE STUDIES USING C-BAND RADARS**

STUDIES PERFORMED UNDER CONTRACTS NAS6-1467 AND NAS6-1628

**CASE FILE  
COPY**

By:

**Wolf Research and Development Corporation**

**Range Engineering Department**

**Riverdale, Maryland**

And:

**RCA Corporation**

**Missile and Surface Radar Division**

**Moorestown, New Jersey**

Prepared for:

**NATIONAL AERONAUTICS AND SPACE ADMINISTRATION**

**WALLOPS STATION**

**WALLOPS ISLAND, VIRGINIA 23337**

**October 1972**

GEOS-II C-BAND RADAR  
SYSTEM PROJECT

FINAL REPORT

MARINE STUDIES  
USING  
C-BAND RADARS

STUDIES PERFORMED  
FOR  
NASA/WALLOPS STATION  
UNDER  
CONTRACTS NAS6-1467 AND NAS6-1628  
NASA Technical Monitor - H.R. Stanley

BY

WOLF RESEARCH AND DEVELOPMENT CORPORATION  
Range Engineering Department  
Riverdale, Maryland  
and  
RCA CORPORATION  
Missile and Surface Radar Division  
Moorestown, New Jersey

October 1972

# TABLE OF CONTENTS

	<u>PAGE</u>
1.0 INTRODUCTION	1
2.0 TASK OBJECTIVES	2
3.0 METHOD OF APPROACH	4
3.1 ANALYSIS OF MOVING TRACKER POSITIONING	4
3.1.1 Range Measurement Relations for a Moving Tracker	5
3.1.2 Effects of SINS Errors on Moving Tracker Ranges	12
3.2 PROGRAM DEVELOPMENT	15
3.2.1 A/Omega Modifications	15
3.2.2 ORAN Modifications	16
4.0 EXPERIMENTAL RESULTS	20
4.1 DATA SELECTION	21
4.1.1 Use of Angle Data	21
4.1.2 Use of Raw Range Data	22
4.1.3 Selection of Data Spans	22
4.2 ORBIT ERROR EFFECTS ON SHIP POSITIONING	23
4.3 DOCKSIDE TESTS	26
4.4 AT SEA TEST RESULTS	31
4.4.1 One Pass Solution - Revolution 7991	31
4.4.2 One Pass Solution - Revolution 8004	35
4.4.3 Two Pass Solution - Revolutions 8003-8004	38

TABLE OF CONTENTS (Cont.)

	<u>PAGE</u>
4.4.4 Two Pass Solution - Revolutions 8010-8011	43
4.4.5 Range Bias Estimation	45
5.0 CONCLUSIONS AND RECOMMENDATIONS	47
REFERENCES	49
APPENDIX A SHIP DATA TRANSFORMATIONS FOR MOVING TRACKER IMPLEMENTATION	A-1
APPENDIX B PROPAGATION OF ERRORS IN AN INERTIALLY GUIDED SURFACE VEHICLE WITH APPLICATION TO TRACKING SHIP ERROR REDUCTION	B-1

LIST OF TABLES

		<u>PAGE</u>
Table 1	Effects of Orbit Uncertainty on One Revolution (Geos-II Rev 7991) Ship Positioning Accuracy	24
Table 2	Effects of Orbit Uncertainty on Two Revolution (Geos-II Revs 8003-8004) Ship Positioning Accuracy	25
Table 3	Dockside Ship Test (Geos-II Revs 7972-7973) NAD-27 Positions	28
Table 4	At Sea Ship Test (Geos-II Rev 7991)	32
Table 5	At Sea Ship Test (Geos-II Rev 8004)	36
Table 6	At Sea Ship Test (Geos-II Revs 8003-8004)	39
Table 7	At Sea Ship Test (Geos-II Revs 8010-8011)	44
Table 8	Estimated Radar Biases	46

## LIST OF FIGURES

		<u>PAGE</u>
Figure 1	Residuals for GEOS-II Rev 7972	29
Figure 2	Residuals for GEOS-II Rev 7973	30
Figure 3	Ship Range Residuals for GEOS-II Rev 7991	34
Figure 4	Ship Range Residuals for GEOS-II Rev 8004	37
Figure 5	Ship Range Residuals for GEOS-II Revs 8003 and 8004	40
Figure 6	Ship Range Residuals for GEOS-II Revs 8010 and 8011	41

## SECTION 1.0 INTRODUCTION

One of the secondary objectives of the GEOS- II C-Band Systems Project is to study the feasibility of using geodetic satellites to both evaluate shipborne instrumentation and to determine ship positions in broad ocean areas. The purpose of this task is to determine whether shipborne C-Band radar tracking, in conjunction with ground based tracking, is sufficiently accurate to provide instrumentation evaluation and ship position estimates. Data from several Apollo tracking ships, in particular the USNS Vanguard, was made available for this effort. A series of tests, using the USNS Vanguard, were carried out in the Port Canaveral and Bahama Acoustic Transponder Array Areas. The major portion of the analyses reported in this document are the result of preliminary investigations using the data from these tests.

The use of shipborne tracking will be useful in several geodetic and geophysical areas provided the reduction techniques prove to be feasible and the data of geodetic quality. For example, the mapping of areas in the vicinity of geodetic anomalies could be performed by radar equipped vessels, the location of acoustic transponders for use as geodetic reference sources can be accomplished in areas not visible from shore, high accuracy navigation updating of position can be accomplished for mapping and geophysical experimentation at sea, and the use of shipborne trackers as auxiliary or complementary stations in geodetic network investigations can be accomplished.

SECTION 2.0  
TASK OBJECTIVES

In order to satisfy the overall project objectives, it has been necessary to establish a set of task objectives designed to insure that the information flow for the task would be efficient, meaningful and useful. Briefly stated the task objectives are:

- a. To understand the data furnished by the shipborne radar. This includes the corrections applied by the ship, the transformations performed on the raw data to convert it to deck coordinate data, the format of the data and what type supporting data is normally furnished by the ship.
- b. To properly calibrate the shipborne radar data to remove zero set errors.
- c. To design and implement a set of pre-processing procedures to apply the proper corrections to the shipborne radar data and to provide meaningful navigation system information in a "moving tracker" position estimation scheme.
- d. To design, checkout and implement a computer program capable of estimating the epoch position of a moving tracker.
- e. To reduce and analyze actual tracking data under a variety of field conditions to demonstrate the feasibility of the ship

positioning technique and to pinpoint actual and/or potential problem areas in the technique.

- f. To devise mathematically and physically sound techniques for properly accounting for sources of error found in e.
- g. To provide a qualitative assessment of the technique along with supporting justification for accuracy estimates, and proposed further studies.

The following sections of this report describe the approaches used to satisfy these objectives. Problem areas are defined in detail and the techniques used to overcome these problems are described. The results of both simulation and live test analysis and reductions are presented with qualitative assessments of the results.

SECTION 3.0  
METHOD OF APPROACH

3.1 ANALYSIS OF MOVING TRACKER POSITIONING

The determination of the position of a ship, or other moving tracker, using radar tracking of a satellite is very similar in concept to that of positioning land based radars. A satellite orbit is determined with the help of other stations tracking the same satellite during approximately the same time period. Simultaneously, a position for the ship is estimated such that the ship radar measurements best fit the determined orbit. In application, however, there are a number of factors which complicate the problem and significantly affect the accuracy with which ship position at any time can be estimated.

The following factors distinguish the problem of position estimation for a moving radar tracker from that for a fixed tracker:

- (1) The variation in ship position from that at a reference time must be accounted for at some stage of the data processing.
- (2) The difficulty in accounting for short period variations in the orientation of the radar mount due to ship roll, pitch and heading variations makes azimuth and elevation angle data essentially useless at geodetic satellite ranges for the position determinations of interest. Range data is thus the only usable radar measurement.

- (3) For most applications, only a limited time and number of satellites are available for use in the ship position estimation. The large number of crossing arcs on all sides of the station often available for estimating land based stations is conceivably available for the positioning of permanent geodetic control points. This application is, however, somewhat beyond the scope of the present report.
  
- (4) Radar calibration on a ship at sea is more difficult to obtain and maintain than for a land based radar. Unless very exacting calibration and operating procedures are followed, range biases of magnitudes varying from one satellite pass to the next may thus be expected.

Taken together, all these factors require that the problem of precise ship positioning be treated considerably differently from land based station positioning. The analytical differences will be treated in the following two sub-sections.

### 3.1.1 Range Measurement Relations for a Moving Tracker

There are a number of means potentially available for determining the position of the VANGUARD at various times while at sea. Those for which some data has been available on tests to date include:

1. C-Band radar track of GEOS-II (convertible into position).

2. LORAC-B, LORAC-A
3. SRN-9 (navigation satellite)
4. Star tracker
5. SINS, Mark-19
6. Acoustic transponder (convertible into position)

In general, all these methods individually have very serious limitations, particularly in accuracy. In addition, some are available only at special times, in certain geographic locations, or under clear weather conditions. Only the SINS system (and, under certain conditions, the acoustic transponder positioning system) is able to provide a near continuous record of ship position. Over a "short" period, its accuracy is potentially very accurate. Over a period of many hours, its accuracy becomes degraded below that of several other methods of positioning.

The positioning of a ship using C-Band radar data alone is an instantaneous fix only if all three measurement types recorded by the radar (R, A, E) are actually used. Biases in the angle measurements, however, make this mode of positioning very inaccurate. Such data has had very limited utility for results quoted in this report. The uses which have been made of angle data have been only for transformation of range data and will be briefly discussed in connection with the dockside test results presented in Section 4.3.

Using radar range data without angle data for ship position determination required data to be taken at more than one time, and required horizontal motion of the ship to be accounted for between range measurements. The use of the SINS system as the method for obtaining this relative ship movement is the logical choice in view of its availability, its accuracy, and its continuity. Accordingly, we will assume that SINS data can be used to relate ship coordinates  $(\phi, \lambda)$  at any time  $t$  to ship coordinates  $(\phi_0, \lambda_0)$  at some earlier time  $t_0$ . A restriction must be that  $t-t_0$  not be too large. For present purposes, it will be assumed that  $t-t_0$  may reach approximately 2 hours, so that two passes of satellite tracking data may be used in the same data reduction, with all ship positions accurately related to the ship position at the reference time  $t_0$ . The desirability of using two passes of tracking data is intuitively obvious merely from the fact that, in general, one satellite track is east of the ship and the other is west of the ship. Barring the simultaneous introduction of additional error sources, the geometry provided by the two passes over and above a single pass cannot but help provide a stronger ship position. Nevertheless, single pass solutions will not be ruled out of consideration.

The data reduction for the moving tracker position estimation must then take into account that the tracker may be at any position relative to its reference time ( $t_0$ ) position, but with the change in position available in SINS coordinates which may be taken to be latitude, longitude, and height above some spheroid  $(\phi-\phi_0, \lambda-\lambda_0, H-H_0)$ . In addition, the processing must take into account the physical separation of the C-band radar from the SINS binnacle to which the SINS position is referenced. The latter processing

is a transformation of coordinates incorporating both the translation and rotation of the true radar coordinates from those of the SINS binnacle. The transformation is discussed in detail in Appendix A and takes into account the flexure of the ship for which measurement data is available. The transformation requires the use of SINS heading data but makes no use of the radar angle measurements.

In essence, the SINS and ship flexure data are used to relate the position of the radar at any time  $t$  to its position at the reference time  $t_0$ . Changes in radar coordinates are thus not simply differences between SINS coordinates, but rather between radar coordinates obtained through transformations of SINS data. This distinction is of particular importance if there is a change in ship heading during a track.

The range measurement made from the moving tracker at time  $t$  can be expressed functionally as:

$$R = \sqrt{(X-x)^2 + (Y-y)^2 + (Z-z)^2} \quad (3-1)$$

where

$X, Y, Z$  are ship earth centered fixed coordinates at time  $t$ .

$x, y, z$  are satellite earth centered fixed coordinates at time  $t$ .

The possible existence of range biases or other such systematic errors may be treated in the same way as for a fixed tracker and may thus be ignored in the present context. In order to make use of the "known" relative movement of the ship from its reference position, we note that a given  $(\phi, \lambda, H)$  is equivalent to an  $(X, Y, Z)$  with the transformation requiring only the spheroid parameters. The relation of the range to the initial position of the ship, which is to be estimated, is somewhat more involved. Using matrix notation, the variation in a computed range measurement with a change in the reference position of the ship may be expressed as

$$\delta R = \begin{bmatrix} \frac{\partial R}{\partial X} & \frac{\partial R}{\partial \phi} & \frac{\partial R}{\partial \lambda} & \frac{\partial R}{\partial H} \end{bmatrix} \begin{bmatrix} \delta X_0 \\ \delta \phi_0 \\ \delta \lambda_0 \\ \delta H_0 \end{bmatrix}$$

where all symbols on the right hand side now denote matrices or vectors,

$$\begin{bmatrix} \frac{\partial X}{\partial \phi} \\ \frac{\partial Y}{\partial \phi} \\ \frac{\partial Z}{\partial \phi} \end{bmatrix} \rightarrow \begin{bmatrix} \frac{\partial X}{\partial \phi} & \frac{\partial X}{\partial \lambda} & \frac{\partial X}{\partial H} \\ \frac{\partial Y}{\partial \phi} & \frac{\partial Y}{\partial \lambda} & \frac{\partial Y}{\partial H} \\ \frac{\partial Z}{\partial \phi} & \frac{\partial Z}{\partial \lambda} & \frac{\partial Z}{\partial H} \end{bmatrix} ; \quad \begin{bmatrix} \frac{\partial \phi_0}{\partial X_0} \\ \frac{\partial \phi_0}{\partial Y_0} \\ \frac{\partial \phi_0}{\partial Z_0} \end{bmatrix} \rightarrow \begin{bmatrix} \frac{\partial X_0}{\partial \phi_0} & \frac{\partial X_0}{\partial \lambda_0} & \frac{\partial X_0}{\partial H_0} \\ \frac{\partial Y_0}{\partial \phi_0} & \frac{\partial Y_0}{\partial \lambda_0} & \frac{\partial Y_0}{\partial H_0} \\ \frac{\partial Z_0}{\partial \phi_0} & \frac{\partial Z_0}{\partial \lambda_0} & \frac{\partial Z_0}{\partial H_0} \end{bmatrix}^T$$

$$\frac{\partial \phi}{\partial \phi_0} \rightarrow \begin{bmatrix} \frac{\partial \phi}{\partial \phi_0} & \frac{\partial \phi}{\partial \lambda_0} & \frac{\partial \phi}{\partial H_0} \\ \frac{\partial \lambda}{\partial \phi_0} & \frac{\partial \lambda}{\partial \lambda_0} & \frac{\partial \lambda}{\partial H_0} \\ \frac{\partial H}{\partial \phi_0} & \frac{\partial H}{\partial \lambda_0} & \frac{\partial H}{\partial H_0} \end{bmatrix}$$

$$\frac{\partial R}{\partial X} \rightarrow 1/R \begin{bmatrix} X-x \\ Y-y \\ Z-z \end{bmatrix}^T, \quad \delta X_0 \rightarrow \begin{bmatrix} \delta X_0 \\ \delta Y_0 \\ \delta Z_0 \end{bmatrix} \quad (3-3)$$

From the assumption that the SINS data provides good measurements of the change in latitude, longitude, and height, we have the relations

$$\begin{aligned} \phi &= \phi_0 + \Delta\phi \\ \lambda &= \lambda_0 + \Delta\lambda \\ H &= H_0 + \Delta H \end{aligned} \quad (3-4)$$

With  $\Delta\phi$ ,  $\Delta\lambda$ , and  $\Delta H$  constants, the matrix  $\frac{\partial \phi}{\partial \phi_0}$  reduces to the unit matrix.

The other partial derivative matrices are calculated from the following relations for transforming geodetic coordinates to earth centered fixed coordinates:

$$\begin{aligned}
 X &= \cos \phi \cos \lambda [H + a_e (1-e^2 \sin^2 \phi)^{-1/2}] \\
 Y &= \cos \phi \sin \lambda [H + a_e (1-e^2 \sin^2 \phi)^{-1/2}] \\
 Z &= \sin \phi [H + a_e (1-e^2)(1-e^2 \sin^2 \phi)^{-1/2}]
 \end{aligned}
 \tag{3-5}$$

where

$a_e$  = semi-major axis of the adopted spheroid for the earth.

$e$  = eccentricity of this spheroid.

The matrix  $\frac{\partial X}{\partial \phi}$  is obtained by straightforward differentiation of (3-5) and will not be given here. The matrix  $\frac{\partial X_0}{\partial \phi_0}$  is identical in form.

The computation of the range measurement expressed by Eqn. (3-1) and the partial derivative matrices of Eqn. (3-2) constitute all necessary calculations that are distinct from those which are necessary for estimating the position of a fixed tracking station using range data. In addition, it may be noted that the basic mathematical expressions used are identical to those for a fixed station.

### 3.1.2 Effects of SINS Errors on Moving Tracker Ranges

The analysis of the preceding section has been based on the assumption that the SINS determination of relative latitude, longitude, and height has negligible error. Since this assumption is only a convenient, and in some cases necessary, approximation, it is highly desirable to be able to recognize the presence of SINS errors in reduced data. It is also desirable, if at all possible, to be able to effectively account for SINS errors or to design tests such that SINS errors are minimized.

A brief analysis of the source and form of SINS errors is presented in Appendix B for several types of ship motion and SINS operation. Some of the conclusions which may be drawn from this analysis are:

1. Ship motion during or between radar satellite tracks does affect SINS positioning errors, but the functional form for the errors is not appreciably affected.
2. Physically distinct error sources produce effects which, using data over two 10-15 minute segments, separated by a two hour period, would be expected to be inseparable on the basis of their effects on ship position error.

3. SINS position errors, though arising from several distinct physical sources, can be approximately modeled by the expressions:

$$\Delta\phi = A_1 + B_1 t + C_1 \sin(\omega t + \gamma_1)$$

(3-6)

$$\Delta\lambda = A_2 + B_2 t + C_2 \sin(\omega t + \gamma_2)$$

where the A's, B's, C's, and  $\gamma$ 's are all independent constants.  $\Delta\phi$  and  $\Delta\lambda$  are errors in latitude and longitude,  $t$  is elapsed time from some arbitrary reference time, and  $\omega$  is the Schuler frequency for a SINS system operating in an undamped mode. When damping is used, the frequency  $\omega$  is increased as a function of the degree of damping.

The effects of the SINS error model parameters on range measurements enter through the (X,Y,Z) coordinates of Eqn. (3-1), which in turn depend upon ( $\phi$ ,  $\lambda$ , H). The SINS error model parameters enter the last set of coordinates in a linear manner according to Eqn. (3-6). Let  $\Delta\alpha$  be the error in one of the SINS error model parameters. Then the range measurement is affected by the amount

$$\delta R = \frac{\partial R}{\partial X} \frac{\partial X}{\partial \phi} \frac{\partial \phi}{\partial \alpha} \delta \alpha$$

(3-7)

The vector  $\frac{\partial R}{\partial X}$  and the matrix  $\frac{\partial X}{\partial \phi}$  are given by Eqn. (3-3).

If we let  $\alpha$  be the parameter  $B_1$ , e.g., the vector  $\frac{\partial \phi}{\partial \alpha}$

becomes:

$$\frac{\partial \phi}{\partial B_1} = \begin{bmatrix} t \\ 0 \\ 0 \end{bmatrix} \quad (3-8)$$

Partials with respect to the other parameters may be obtained using (3-6) in a similar manner.

For error analyses, which normally require only partial derivatives without the need for actual residuals, the parameter partial derivative expressed by

$$\frac{\partial R}{\partial \alpha} = \frac{\partial R}{\partial X} \frac{\partial X}{\partial \phi} \frac{\partial \phi}{\partial \alpha} \quad (3-9)$$

is the only quantity needed in order to investigate the effects of SINS errors on data reductions which use moving tracker data. The manner in which the SINS parameter error analysis can be implemented will be discussed below.

## 3.2 PROGRAM DEVELOPMENT

Analysis of moving tracker data used for ship position estimation required modifications to two large scale computer programs: the A/Omega orbital data reduction program and the ORAN orbital error analysis program. Although the two programs model the same data reduction process, the functions which the programs serve are, although complementary, quite distinct. The modifications to the two programs are thus completely different and will be discussed separately.

### 3.2.1 A/Omega Modifications

The nature of the modifications required for A/Omega to incorporate moving tracker data under the assumptions made above are of two types:

#### 1. Input Modifications

In order for the A/Omega program to be able to recognize and use moving tracker data properly, the data input format was modified to provide: an indicator that the tracker was a moving tracker type; and the changes in ship radar position ( $\Delta\phi$ ,  $\Delta\lambda$ ,  $\Delta H$ ) from that at some reference time. This reference time was basically arbitrary, but was chosen to be the time of the first usable data point of the satellite pass (or the first satellite pass if two successive satellite passes were tracked).

#### 2. Computations of updated station position.

The computation of measurement residuals and partial derivatives requires the current position of the ship for use in Eqns. (3-1) and (3-3). The A/Omega program was originally designed to operate with station positions which changed only as a result of a least squares adjustment based on satellite tracking data. Consequently, the program had to be reconfigured to compute a new station position and rotation matrices for each data point. Eqns. (3-5) are used to compute the new station position and the rotation matrices are computed using (3-3). The initial, or reference, position of the moving tracker must be retained in core, adjusted at the end of each iteration, and used as the starting position at the beginning of the next iteration.

No capability for any SINS error model parameter recovery was incorporated into A/Omega, since it was not clear that sufficient data existed for the recovery of any such parameters. The normal program recoveries of measurement biases and station timing errors were retained.

### 3.2.2 ORAN Modifications

To investigate the effects of SINS errors on A/Omega reductions of moving tracker data, the ORAN program was modified for the computation of partial derivatives of range measurements with respect to SINS error model parameters. The parameters investigated are based on Eqn. (3-6) which may be written as:

$$\Delta\phi = (A_1 - C_1 \sin\gamma_1) + B_1 t + (C_1 \cos\gamma_1) \sin \omega t + (-C_1 \sin\gamma_1)(1 - \cos \omega t)$$

$$\Delta\lambda = (A_2 - C_2 \sin\gamma_1) + B_2 t + (C_2 \cos\gamma_1) \sin \omega t + (-C_2 \sin\gamma_2)(1 - \cos \omega t)$$

Since all the parameters are arbitrary anyway, these error expressions can be written equally well as

$$\Delta\phi = A_1 + B_1 t + C_1 \sin \omega t + D_1 (1 - \cos \omega t) \tag{3-10}$$

$$\Delta\lambda = A_2 + B_2 t + C_2 \sin \omega t + D_2 (1 - \cos \omega t)$$

The partial derivatives incorporated into ORAN are the partials of range measurements with respect to the A, B, C, and D parameters of Eqn. (3-10). The particular form of Eqn. (3-10) is chosen such that the constant terms will be the position errors at the reference time (t=0).

The computation of range partial derivatives with respect to SINS error model parameters then utilizes Eqns. (3-9) and (3-10). Due to the relatively small movement of the ship throughout the total tracking period, it is possible to make approximations in Eqn. (3-9) which considerably simplify the necessary program modifications. In particular, we can set

$$\frac{\partial R}{\partial X} \frac{\partial X}{\partial \phi} \approx \frac{\partial R}{\partial X_0} \frac{\partial X_0}{\partial \phi_0} \tag{3-11}$$

Since these partials are already calculated as a part of the station position adjustment simulation, the only additional computations needed are the  $\frac{\partial \phi}{\partial \alpha}$  type calculations based on Eqn. (3-10). These partials are:

$$\frac{\partial \phi}{\partial A_1} = \frac{\partial \lambda}{\partial A_2} = 1$$

$$\frac{\partial \phi}{\partial B_1} = \frac{\partial \lambda}{\partial B_2} = t$$

$$\frac{\partial \phi}{\partial C_1} = \frac{\partial \lambda}{\partial C_2} = \sin \omega t$$

$$\frac{\partial \phi}{\partial D_1} = \frac{\partial \lambda}{\partial D_2} = 1 - \cos \omega t$$

(3-12)

These expressions are simple functions of elapsed time.

The ORAN program also required, of course, input modifications to request the SINS error model parameters. It was then capable of computing the effects of SINS errors on:

1. Adjusted ship range biases.
2. Adjusted ship position.
3. Ship range residuals after the least squares fit of the range data to the satellite orbit adjusting for ship position.

The program output was then usable for analyzing the A/Omega data reduction results to determine the amount and type of SINS errors actually present in the data.

SECTION 4.0  
EXPERIMENTAL RESULTS

The use of shipborne radar data for precise ship positioning has been tested in essentially three phases:

1. Dockside testing to validate the techniques being used in the absence of ship motion and with a known position of the ship. These tests used orbits determined by land based stations and tracking geometry similar to that planned for at sea tests. The dockside tests thus provided a checkout of data handling techniques and gave a ship position whose accuracy could be checked. The dockside accuracy should be approximately equaled at sea except for SINS errors and possibly degraded radar calibration.
  
2. At sea testing with results checked by analysis of ship range residuals and comparison of estimated ship position with that obtained from independent systems such as LORAC. The results obtained here should indicate the accuracy achievable with the SINS data for relative positioning accepted with no attempt at correction or improvement. Since SINS performance can be somewhat variable, some care must be taken in extrapolating results based on a limited number of tests.
  
3. Analysis of at sea tests to determine whether effective improvements can be made in the SINS data which lead to improved positioning capability. For the most part, this analysis consists of comparing data reduction results with the ORAN simulations of the data reduction, and propagating SINS errors into the adjusted parameters and measurement residuals.

The results from these three phases should provide estimates of ship positioning accuracies currently achievable, together with an indication of those procedural and data reduction changes most likely to improve the results of future tests.

#### 4.1 DATA SELECTION

The data selected for the ship positioning studies consisted of "raw" range data from one and two (successive) passes of GEOS-B. The reasons for these choices are given in the following sub-sections.

##### 4.1.1 Use of Angle Data

Azimuth and elevation measurements, although made by the ship radar, provide position measurements grossly inferior to the range measurement. A low angle noise level of 10 arc seconds corresponds, for example, to a position error of about 100 meters at typical GEOS-B ranges. Biases would be expected to be several times this value because of the difficulty in angle calibration. In addition, the removal of ship motion (pitch and roll) cannot be expected to be done without the introduction of appreciable error. On the other hand, the radar range noise level is on the order of two meters, and its bias should be largely removable even for at sea calibrations. Given the exercise of sufficient geometry, range data alone is quite capable of determining all three coordinates of ship position. Ship angle data was therefore not used for ship position studies except for some range transformations as indicated in Section 4.1.2 and 4.3.

#### 4.1.2 Use of Raw Range Data

In order to be able to provide data for external use in fixed tracker data reductions, the ship borne computer possesses the capability of transforming (R,A,E) measurements to the corresponding measurements for a fixed tracking point. This transformation requires two types of input: the location of the ship (or radar) relative to the fixed tracking point; and the three coordinates of position of the satellite. The first of these inputs is provided by the SINS position data. The second is provided by the full set of radar measurements (R,A,E) smoothed over some interval using filtering appropriate for a target in orbit. The transformed data is thus affected by SINS errors and radar angle errors (noise and biases) and is acceptable data only if there is no better procedure for handling it. The use of raw data does not eliminate the effects of SINS errors unless there is some auxiliary position measurement available. It does, however, completely eliminate the effects of angle errors since the satellite orbit determined by ground based trackers is effectively used as a basis for the measurement transformation. For these reasons, ship transformed radar data has had very limited use and the raw data has been used instead.

#### 4.1.3 Selection of Data Spans

In all ship position studies made to date, one or two revolutions of satellite tracking data has been used both from land based trackers and from the ship. There are a number of reasons for both using two revolutions and also for limiting the data span to two revolutions. The need for more than one revolution of data is because of the much greater geometry for the ship which the two passes (rather than one) provide, with an associated cancellation of both ship and

land based radar error effects. Two revolutions of land based data should also provide a somewhat more accurate orbit unless a large number of ground stations are tracking during the single revolution case (as was never the case). To extend the tracking period beyond two revolutions means that at least a twelve hour period must be used. Orbit errors can be considerably greater for this period than for the approximately two hour period needed for the two revolutions. In addition, SINS errors become essentially intolerably large. The one pass results are of interest because of the situations in which only one pass of data is available, which is the case with SRN-9 type positioning.

#### 4.2 ORBIT ERROR EFFECTS ON SHIP POSITIONING

One of the limitations on the accuracy with which ship position can be determined using satellite tracking data is the accuracy of the satellite orbit itself. With the satellite well tracked by highly accurate instruments on the ship (e.g., measuring R, A, E), it would be expected that orbit errors would translate one to one into positioning errors. Because of the limited amount and type of good tracking data, together with the nature of the actual orbit errors, there can be a magnification of orbit errors when transformed into tracking station error.

Two station recoveries were simulated using the ORAN program for the purpose of estimating the effects of various orbit error sources on one and two revolution solutions. The orbital solutions were each determined by two ground based radars. The one revolution solution used data from Wallops and Bermuda and the two revolution solution used data from Bermuda and Antigua. The effects of

various ground based tracker errors on the recovered positions will depend somewhat upon the position of the ship relative to each tracking station. The two simulations performed can, however, be considered as reasonably representative of one and two revolution solutions when ship range biases must be estimated on each pass.

Tables 1 and 2 show the effects of postulated station location, range bias, refraction, and geopotential coefficient errors on the one and two revolution ship position recoveries. For the one pass solution, the largest effects are due to ground station biases, for which slightly pessimistic values of 3 meters have been assumed. Geopotential coefficient errors, as might be expected, have a completely negligible effect on this solution. The total uncertainty is approximately 12 m, which is comparable to what can be expected for the positioning of land based stations using multiple passes.

Table 1  
Effects of Orbit Uncertainty on One  
Revolution (Geos B Rev 7991) Ship Positioning Accuracy

Orbit Error Source	Effect (Meters) on	
	Latitude	Longitude
Station Position	.1	1.7
Uncertainty (Bermuda relative to Wallops)	Lat (5m)	1.7
	Lon (5m)	6.6
	Height (5m)	5.3
Ship refraction (10%)	.6	2.0
Geopotential Coefficient (0.25 APL-SAO)	.6	.7
Bermuda Range Bias (3m)	1.4	6.1
Wallops Range Bias (3m)	.5	4.8
TOTAL	3.0	11.5

Table 2  
Effects of Orbit Uncertainty on Two  
Revolution (Geos B Revs 8003-8004) Ship Positioning Accuracy

Orbit Error Source	Effect (Meters) On		
	Latitude	Longitude	
Station Position	Lat (5m)	2.7	0.2
Uncertainty (Bermuda relative to Antigua)	Lon (5m)	2.8	1.4
	Height (5m)	6.5	13.7
Ship Refraction (10%)		2.5	4.2
Geopotential Coefficients (0.25 APL-SAO)		2.8	7.3
Bermuda Range Bias (3m)		7.1	13.0
Antigua Range Bias (3m)		.7	4.3
RSS Effects		11.1	21.2

The effects of radar biases are still the dominant error source for the two pass solution, as shown in Table 2. They are actually somewhat greater than for the single pass solution, although this may be attributed to less favorable geometry for the orbit determination. Geopotential coefficient errors now have a non-negligible effect, since such errors do produce orbit errors of a few meters for a one revolution solution. The total uncertainty of about 24 m is considerably greater than that achievable for ground based stations with good geometrical coverage. The necessity of bias recovery on both passes is largely responsible for the magnitude of 24 m.

### 4.3 DOCKSIDE TESTS

Using two successive GEOS-B tracks by the Vanguard C-band radar with the ship in Port Canaveral, it has been possible to check out the radar and data handling and reduction processes under near ideal conditions. Lack of motion by the ship removed the complications of the moving tracker. And the position of the tracker was tied to a well surveyed point. Position recovery under these conditions should give an indication of the accuracy that should be expected when the ship motion is perfectly taken in account.

Table 1 shows the radar position recovered when tracks of Revolutions 7972 and 7973 were used in conjunction with land-based tracking by Wallops and Bermuda radars. The estimated position, when compared to the survey position also shown in Table 3, shows a difference of only 17 meters. This figure should be considered a measure of the accuracy of the estimated position relative to Wallops and Bermuda.

For both radar passes, independent radar range biases were estimated along with the ship position. Biases of -67 and -17 meters were recovered, indicating both significant biases and biases which differ between passes.

The ship radar and land based radar residuals (differences between the observed ranges and the calculated ranges to the fitted orbit) for Revolutions 7972 and 7973 are shown in Figures 1 and 2, respectively. The raw radar range residuals are denoted by ISTA19. The residuals denoted by ISTA66 refer to the low speed data transformed by the ship computer as discussed in Section 4.1.2. The

trends in these residuals are an indication that something was wrong in the transformation process. The ISTA19 residuals seem quite comparable to the land-based radar range residuals.

In addition to the Vanguard dockside tests discussed above, in port reductions have also been made of a single revolution of data for an Apollo tracking ship in the Sydney, Australia, harbor. The results of this test have been reported in Reference 1 and show recovery accuracy somewhat less, but still on the same order as is indicated by Table 3.

TABLE 3

DOCKSIDE SHIP TEST

GEOS-B REVS 7972 - 7973

NAD-27 POSITIONS

	Adjusted	Survey
Latitude	28° 24' 31.8"	28° 24' 31.4"
Longitude	279° 23' 44.1"	279° 23' 44.5"
Height	7.2 m	14.6 m

Orbit Determination by:

Wallops FPS-16

Bermuda FPQ-6

Bermuda FPS-16

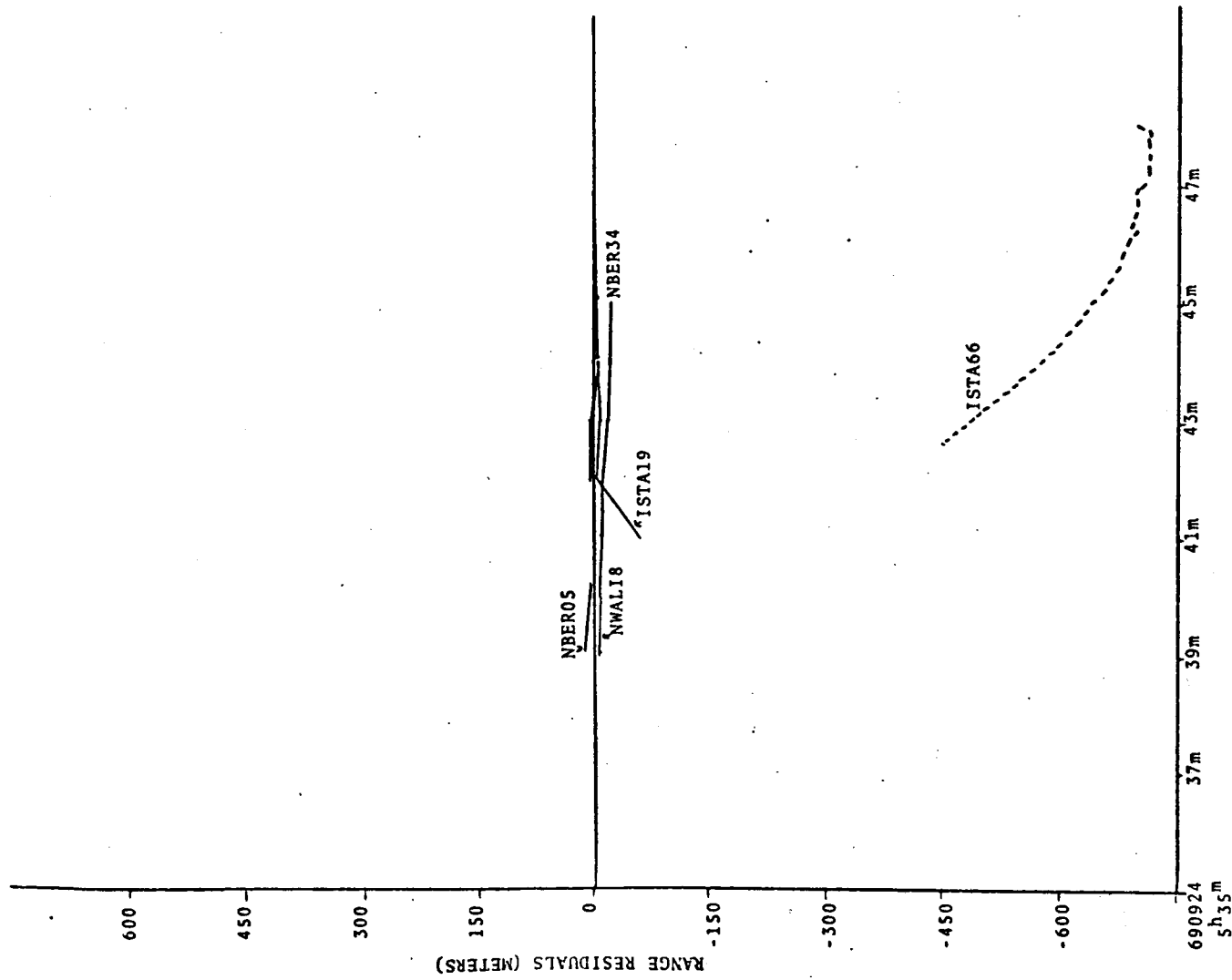


Figure 1. Residuals for GEOS-B Rev 7972

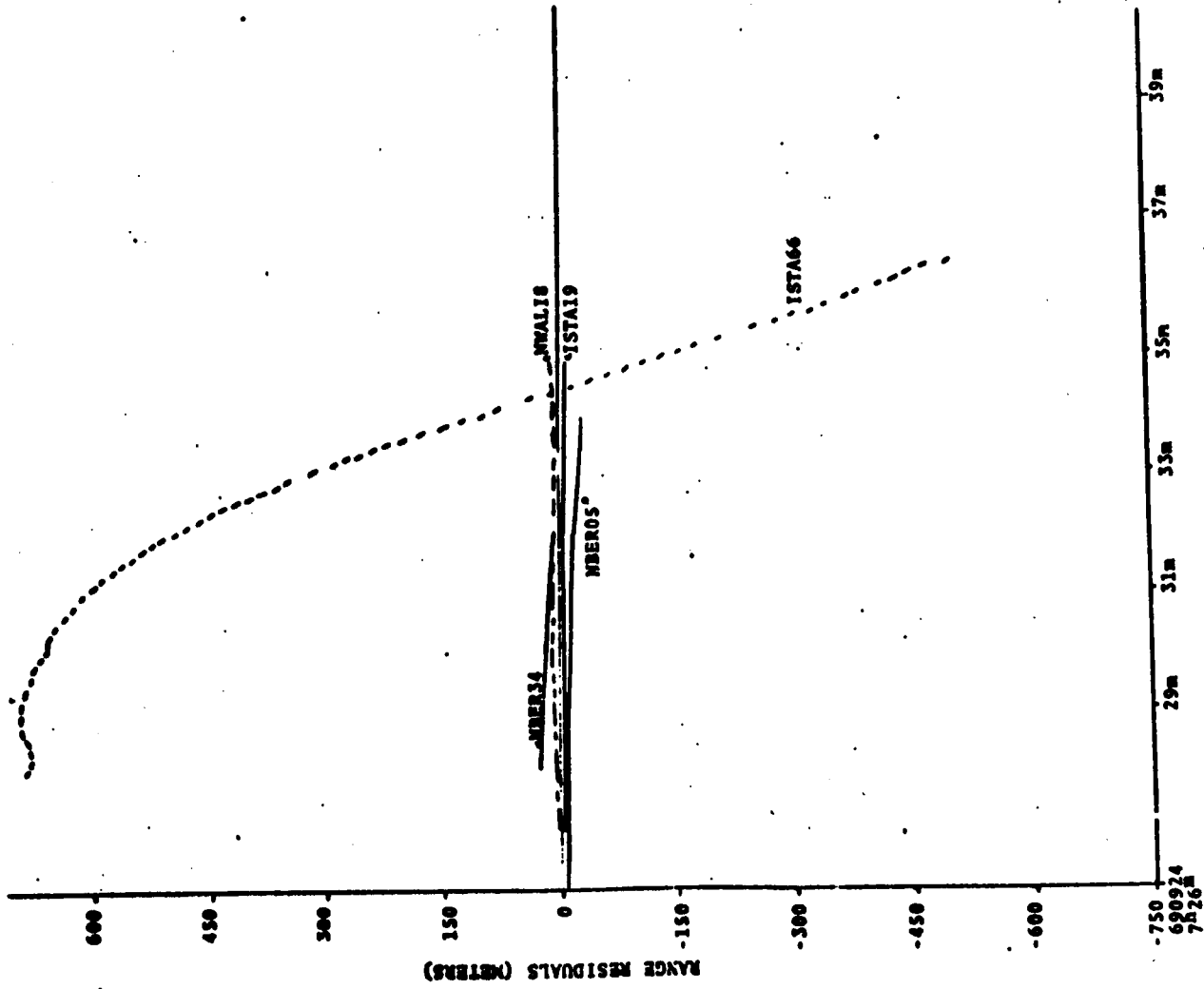


Figure 2. Residuals for GEOS-B Rev 7973

#### 4.4 AT SEA TEST RESULTS

At sea Vanguard tracks on three different days have been reduced, in all cases using the SINS data for relating the position of the ship during track to its position at the beginning of track. When tracks on successive revolutions were available, the initial position used was that at the beginning of the first track.

Results for the three different tests will first be given along with some analysis of the recovered ship positions and the large systematic measurement residuals which were obtained for all at sea tests. In one case, one pass of a two pass test will be reduced separately to see how well the one and two pass solutions agree.

It should be noted that a height recovery was not attempted for any of the at sea tests. This constraint was used because of the limited amount of data on some passes and the necessity for recovery of range biases on all passes. This necessity was indicated by the dockside tests, which showed bias differences on the order of 50 meters from one pass to the next (Section 4.3). At sea type data reductions were attempted with no bias recovery, with generally disastrous results, even when SINS errors were estimated.

##### 4.4.1 One Pass Solution - Revolution 7991

Table 4 gives the estimated ship position at the beginning of track on GEOS-B Revolution 7991. The only available comparison position is the SINS position, also listed in Table 4. Differences are approximately 440 meters in latitude and 30 meters in longitude. A reliable estimate for the accuracy of the SINS position is, however, not available.

TABLE 4  
AT SEA SHIP TEST  
GEOS-B REV 7991

	Latitude	Longitude
SINS a priori	28° 23' 22.4"	280° 15' 18.0"
Adjusted (assuming no SINS error)	28° 23' 38.8"	280° 15' 24.2"
Adjusted (including SINS error adjustment)	28° 24' 56.0"	280° 16' 35.6"

Orbit Determination by:

Wallops FPQ-6

Wallops FPS-16

Bermuda FPS-16

The residuals for the ship range measurements after the ship position (and radar bias) estimation are shown in Figure 3. Residuals for the land based radars were somewhat smaller than the ship residuals and are not shown. The SINS velocity error best accounting for the observed residuals was estimated using the modified ORAN program. Velocity error estimates of

$$\delta V_{\text{East}} = 5.3 \text{ m/sec}$$

$$\delta V_{\text{North}} = 2.8 \text{ m/sec}$$

were found. The effects of this velocity error on the ship range residuals are shown as the solid curve of Figure 3. A pattern quite close to that of the actual residuals is observed.

The estimated initial position of the ship, taking account of the above velocity error, is given in Table 4. It will be noted that the "corrected" position is somewhat farther from the a priori SINS position than was the first estimated position. In itself, this does not necessarily indicate a degradation of the recovered ship position, since the accuracy of the SINS initial position is not known. However, the estimated velocity error is unrealistically large - an indication that the total set of adjusted parameters is somewhat suspect. Further evidence of a weak solution is provided by the high correlation (0.99) between the two velocity components. The weak solution is due to the estimation of

2 components of ship position

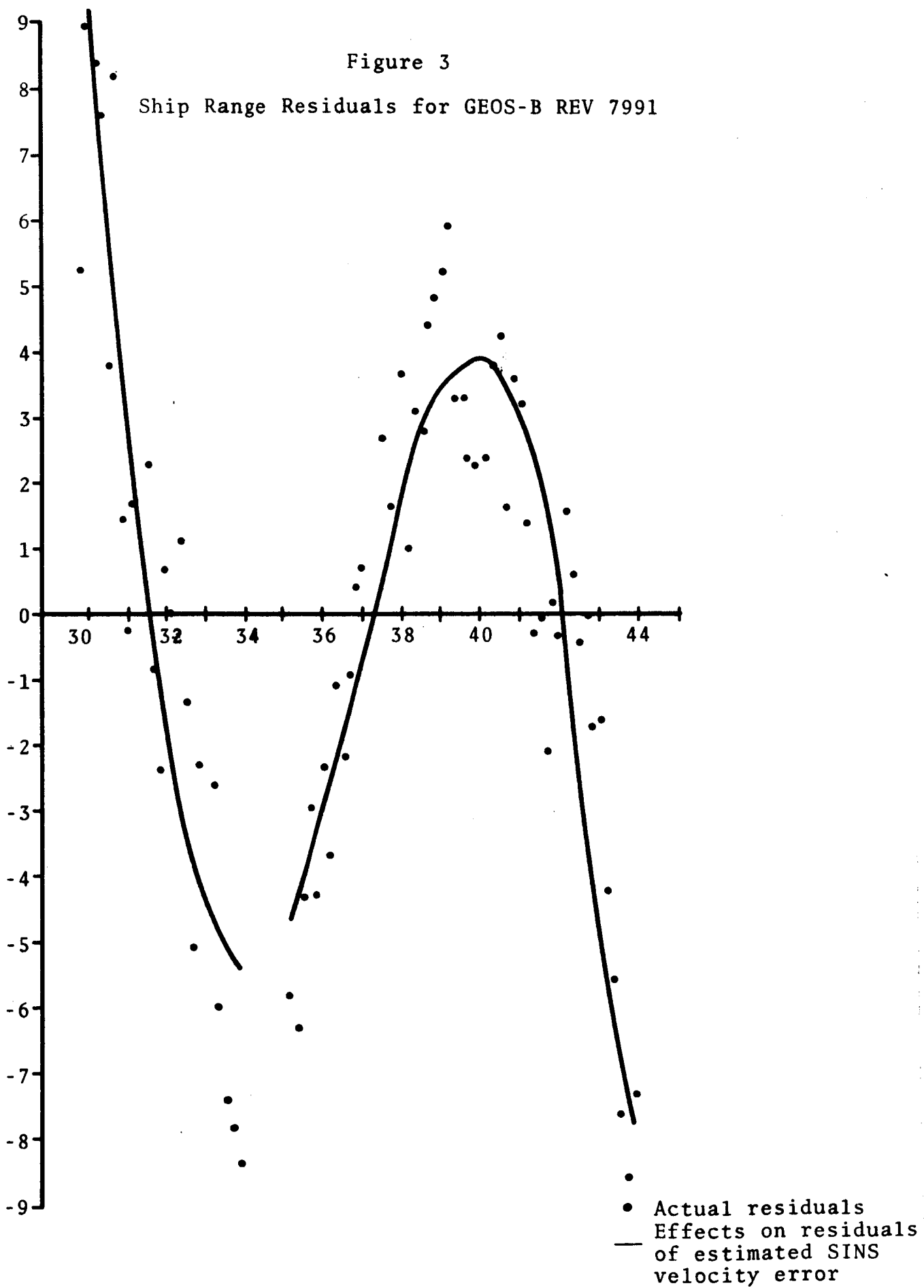
2 components of ship velocity error

1 range bias

using only a limited amount of data. Since the reduction, in the same manner, of data from another single pass radar track

Figure 3

Ship Range Residuals for GEOS-B REV 7991



produced results which look somewhat better, there is a suspicion that the operation of the SINS system during this test may have had problems.

#### 4.4.2 One Pass Solution - Revolution 8004

GEOS-B was tracked by the Vanguard C-Band radar and ground stations on Revolutions 8003 and 8004. For comparison of results with Revolution 7991, the data for 8004 was used alone in a ship positioning solution (both revolutions of ground tracking were used to determine the satellite orbit). The estimated initial position of the ship is shown in Table 5. The time of the reference position was chosen to be prior to Revolution 8003 so that comparisons could be made with the two revolution solution to be discussed below.

In addition to the a priori SINS position for comparison, a LORAC position is also available for this test and is listed in Table 5. The agreement of the estimated latitude with the LORAC latitude is quite poor, differing by about 2500 meters regardless of whether or not SINS errors are estimated. Longitude differences are much smaller, but are still several hundred meters. The SINS velocity error components estimated are

$$\delta V_{\text{West}} = 1.2 \text{ m/sec}$$

$$\delta V_{\text{South}} = 1.0 \text{ m/sec.}$$

As can be seen from the residuals and SINS error effects shown in Figure 4, this velocity error provides a reasonably good explanation for the systematic trends in the ship range

TABLE 5  
 AT SEA SHIP TEST  
 GEOS-II REV 8004

	Latitude	Longitude
SINS a priori	27° 7' 17.5"	283° 39' 0.6"
LORAC	27° 7' 32.0"	283° 38' 53.0"
Adjusted (assuming no SINS error)	27° 9' 12.1"	283° 39' 9.2"
Adjusted (including SINS error adjustment)	27° 9' 7.2"	283° 38' 41.0"

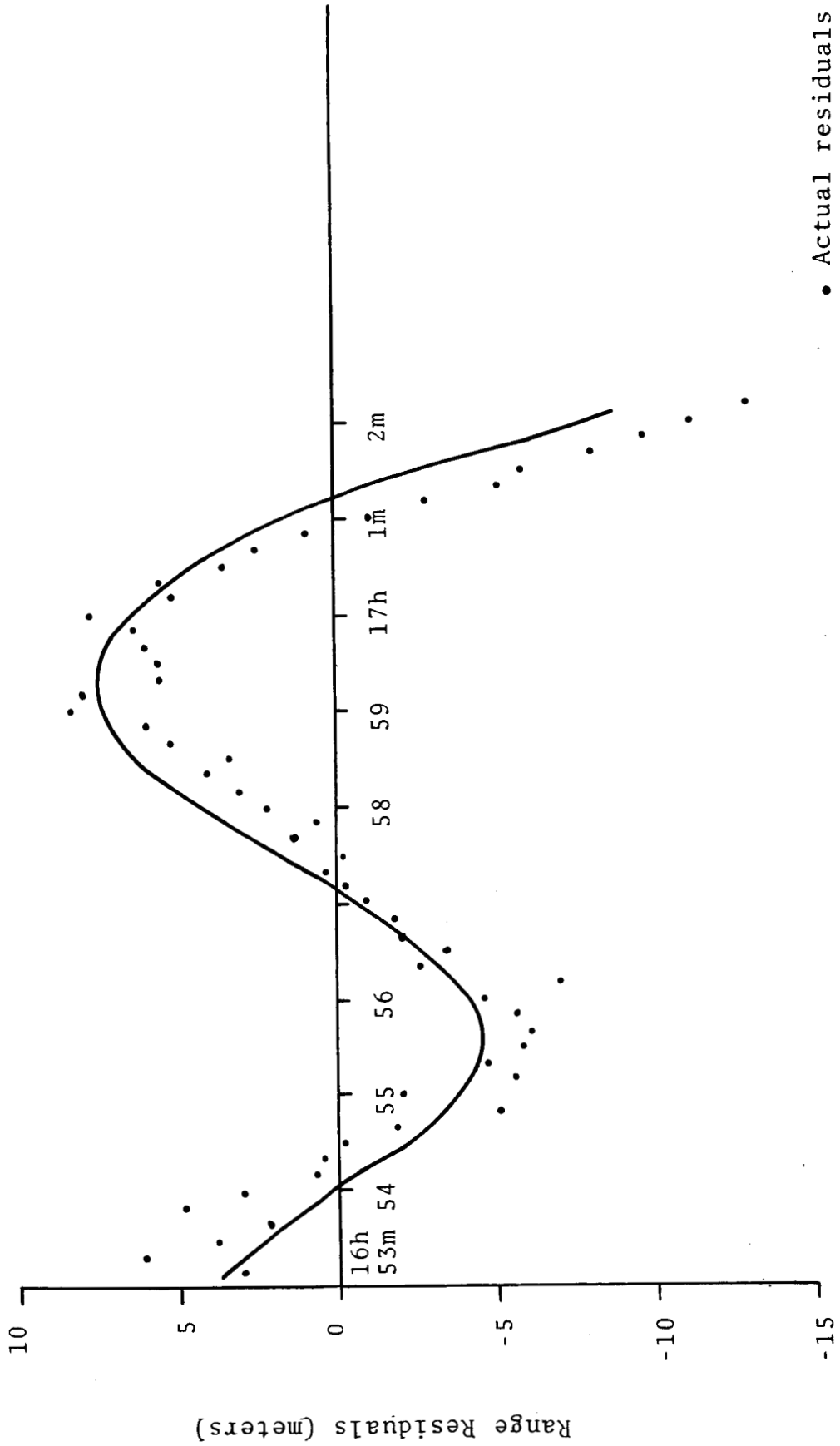
Orbit Determination by:

Bermuda FPS-16

Antigua FPQ-6

Figure 4

Ship Range Residuals for GEOS-B REV 8004



• Actual residuals  
— Effects on residuals of estimated SINS velocity error

residuals. The velocity error estimated, however, is still too large to be physically acceptable. Again, as for Revolution 7991, there are the problems of the adjustment of five parameters using a limited amount of data and a resulting high correlation between the errors in the velocity components.

It should be noted that ship position and velocity errors accumulated between revolutions would affect the comparisons with LORAC given in Table 5, without really affecting the one revolution position determination.

#### 4.4.3 Two Pass Solution - Revolutions 8003-8004

GEOS-II was tracked for only a couple of minutes on Revolution 8003, far less than the approximately ten minutes obtained on some high elevation tracks. Alone, the data is of limited utility for ship positioning. In combination with a good track of Revolution 8004, the data is quite useful because of the additional geometry provided by tracks of both sides of the ship. It is necessary, however, for SINS errors to be either small or well modeled from the beginning of the first revolution track to the end of the second revolution track.

Table 6 shows the adjusted ship position found using data from Revolutions 8003 and 8004. Figure 5 shows the ship range residuals for both revolutions after the ship position and bias (one for each pass) estimations. Comparison with the LORAC position shows the adjusted position to be in error by about 500 m in longitude and 3000 m in latitude. The range residuals remaining after this solution are large (compared to that expected for

TABLE 6  
 AT SEA SHIP TEST  
 GEOS-B REVS 8003 - 8004

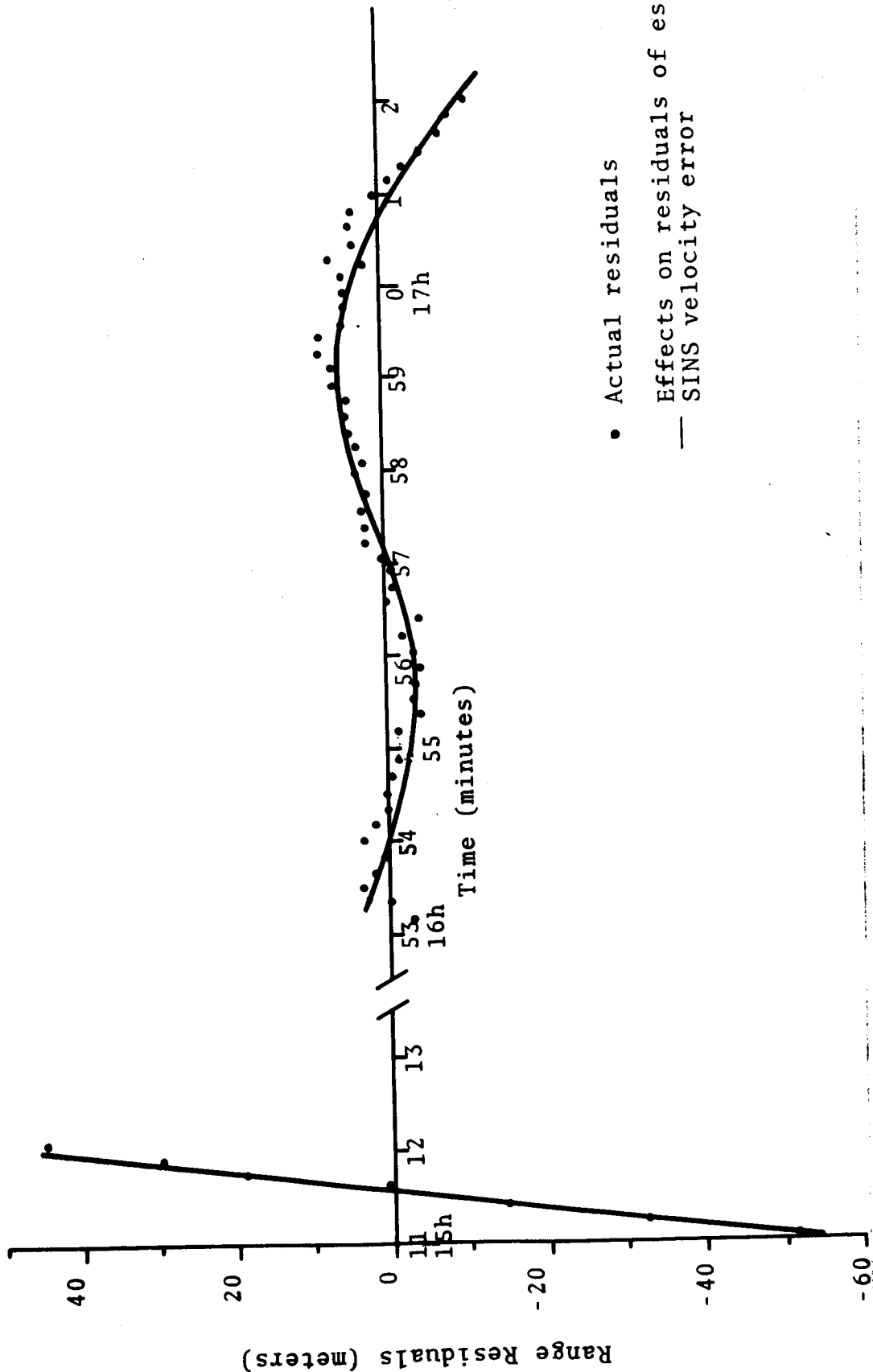
	Latitude	Longitude
SINS	27° 7' 17.5"	283° 39' 0.6"
LORAC	27° 7' 32.0"	283° 38' 53.0"
Adjusted (assuming no SINS error)	27° 9' 12.9"	283° 39' 10.9"
Adjusted (including SINS error adjustment)	27° 7' 23.2"	283° 39' 0.6"

Orbit Determination by:

Bermuda FPS-16

Antigua FPQ-6

Figure 5  
 Ship Range Residuals for GEOS-B REVS 8003 & 8004



- Actual residuals
- Effects on residuals of estimated SINS velocity error

a two revolution orbital fit for ground stations) and trended, particularly for the first revolution.

The SINS velocity errors providing the best fit for the observed residuals are found to be

$$\delta V_{\text{West}} = 0.14 \text{ m/sec}$$

$$\delta V_{\text{South}} = 0.53 \text{ m/sec.}$$

The contributions which these errors make to the actual residuals are also shown on Figure 5. Again, the fit appears quite good. Removing the effects of these velocity errors from the initial ship position, we obtain, as shown in Table 6, agreement with the LORAC position to within less than 300 meters in latitude and approximately 200 meters in longitude.

The adjusted position, including SINS errors, shows closer agreement with the LORAC position than does the a priori SINS position. In addition, the SINS velocity errors estimated are much closer to physically acceptable values than are any of the one revolution solutions. The two revolution solution thus appears far superior to the one revolution solutions, taking into account the necessity for adjusting range biases on each pass and the ship initial position and velocity errors.

The accuracy of the LORAC position was estimated to be approximately 18 meters (antenna separation of approximately 15.24 meters have not been included in Table 6), based on the relative locations of the ship and LORAC transmitting stations (References 2 and 3). The system does qualify as a good standard in this case.

#### 4.4.4 Two Pass Solution - Revolutions 8010-8011

GEOS-B was tracked on Revolutions 8010 and 8011 by the Vanguard radar and two ground based C-band radars. The ship passes were somewhat similar to those for 8003 and 8004, with a short low elevation pass followed by a long high elevation pass. Different ground based radars were used to obtain the satellite orbit. However, the accuracy of the determined orbit should be comparable to that for Revolutions 8003 and 8004. The direction of the satellite passes (North to South instead of South to North) should be insignificant.

The ship position estimated for the beginning of track on Revolution 8010 is given in Table 7. Residuals after the adjustment are shown in Figure 6. The residuals are somewhat similar to those for the 8003 and 8004 passes, with an amplitude approximately twice as large. In addition, there is a data dropout during the middle of the second pass. Correlations of the data dropout with the data quality is unknown. The data reduction assumed the same range bias throughout the second pass, but allowed to vary from that for the first pass.

The SINS velocity error best accounting for the observed residuals was found to be

$$\delta V_{\text{West}} = 0.14$$

$$\delta V_{\text{North}} \approx 0.$$

These errors are physically acceptable and do not result in very large corrections to the ship initial position (compared to the corrections found for Revolution 8003),

TABLE 7

AT SEA SHIP TEST

GEOS-B REVS 8010 - 8011

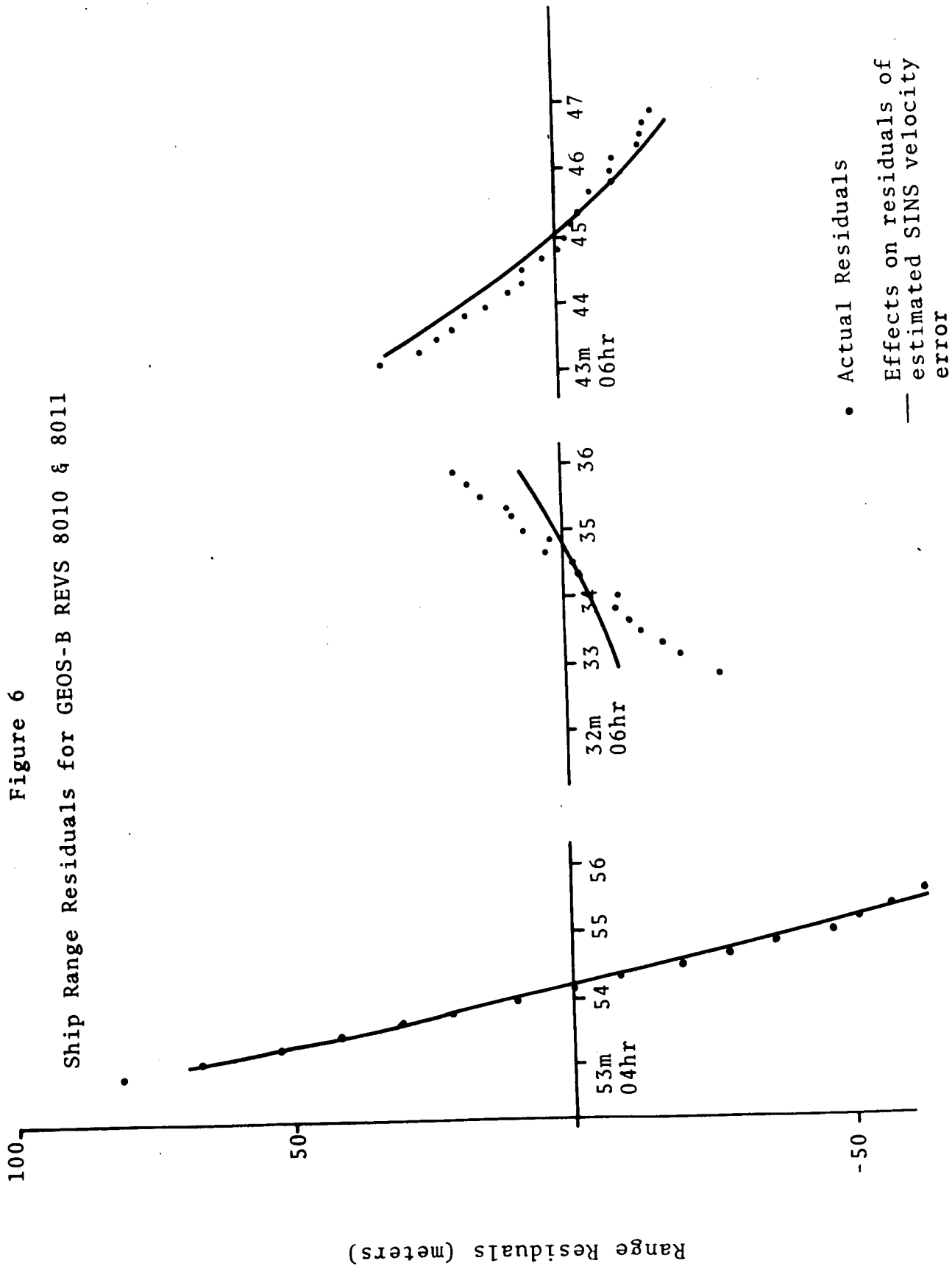
	Latitude	Longitude
SINS a priori	27° 6' 41.8"	283° 38' 10.5"
Adjusted (assuming no SINS errors)	27° 7' 27.1"	283° 37' 35.8"
Adjusted (in- cluding SINS error adjustment)	27° 7' 18.6"	283° 37' 20.9"

Orbit Determination by:

Wallops FPS-16  
Bermuda FPS-16

Figure 6

Ship Range Residuals for GEOS-B REVS 8010 & 8011



as shown in Table 7. The corrections are less than 10 seconds in latitude and about 15 seconds in longitude. However, the above velocity error does not account very well for the actual residuals, as is evident from the curves in Figure 6. In particular, the first part of the second pass does not fit very well at all, and data problems during this period are thus suggested to actually exist. No further analysis of the data on this pass has been made. Different bias levels on the two parts of the second pass is the most probable explanation. However, this would require the estimation of one additional parameter when the solution is already quite weak.

#### 4.4.5 Range Bias Estimation

As has been indicated, range bias recoveries were made in all ship test reductions for each pass. This was considered necessary because of the lack of well established procedures for precise calibration of the ship radar. The biases which were recovered for the various tests are listed in Table 8. Values are given for the SINS error ignored cases and for the SINS error adjusted cases.

In absolute terms, some of these biases are quite large and inconsistent with even a nominal radar calibration. However, the most striking aspect of the Table is the large magnitude of the biases for 8003-8004 with SINS errors ignored, and the degree to which these values are "corrected" when the SINS velocity error adjustment is allowed.

TABLE 8

## Estimated Radar Biases

Revolutions	SINS Error Ignored	SINS Error Adjusted
7991	209 m	241 m
8004	-423 m	-850 m
8003	2885 m	135 m
8004	-404 m	-91 m
8010	-905 m	-968 m
8011	192 m	69 m

SECTION 5.0  
CONCLUSIONS AND RECOMMENDATIONS

The results presented in the preceding sections have shown that C-band radar data from the Vanguard is potentially useful for accurate geodetic positioning provided the relative ship movement can be accurately taken into account. The results and the implications for further analysis may be summarized as follows:

1. A two satellite pass position estimation accuracy on the order of 15 meters is possible using a ship C-band radar when relative ship position between data points is known from other sources.
2. Ship position estimation using SINS data for relative ship motion (and considered to be error free) gives position errors which may exceed 3 km. for a two pass solution.
3. Modeling of SINS errors over a two pass period appears possible, with the solution for speed and heading errors.
4. A much stronger station estimation would be possible if the radar were well calibrated, and no range bias estimation were necessary.
5. One crucial item required in this approach to ship positioning is an independent source of relative position. The use of acoustic transponders for this purpose should be adequate solution under the same conditions.

6. A comparison of SINS positions with LORAC and acoustic transponder positions should help to more clearly identify the magnitude and form of SINS errors.
  
7. The preliminary analyses of the Bahama experiment should be expanded to incorporate the use of acoustic transponder data, and SRN-9 positions, and future experiments planned utilizing the radar calibration information gained during this effort.

## REFERENCES

1. Martin, C.F., N.A. Roy, H.R. Stanley, W.B. Krabill, The Use of Shipborne C-Band Radar Satellite Ranging Data for Accurate Position Determinations in Broad Ocean Areas. Presented at Marine Geodesy Symposium, New Orleans, Louisiana, November 1969. Published in Proceedings.
  
2. Mourad, A.G., A.T. Hopper, D.M. Fubara, G.T. Ruck, Final Report on C-Band Radar Marine Geodesy Experiment Using USNS Vanguard Acoustic Techniques and Results, Batelle Memorial Institute, Columbus Laboratories, July 1970.
  
3. Seiscor Corp., The Application of LORAC to Precision Terrestrial Line Length Measurements and Position Fixing, 1959.

APPENDIX A  
SHIP DATA TRANSFORMATIONS FOR  
MOVING TRACKER IMPLEMENTATION

Let  $X_0$  be the coordinates of the radar relative to a ship origin which should be the center of rotation of the ship. This may be closely approximated by the SINS binnacle. The coordinate system assumed is X toward the bow, Y to starboard, and Z up.

Let us rotate these coordinates into an (ENV) system which has the X axis east, Y north, and Z up. This transformation is for roll, pitch, and heading.

It is more convenient to derive the inverse transformation of heading, pitch, and roll. The heading transformation is a rotation about the Z axis by an amount  $A - \pi/2$  in the negative direction, where A is the heading (or azimuth),

$$\Gamma = \begin{bmatrix} \cos(A - \pi/2) & -\sin(A - \pi/2) & 0 \\ \sin(A - \pi/2) & \cos(A - \pi/2) & 0 \\ 0 & 0 & 1 \end{bmatrix}$$

$$= \begin{bmatrix} \sin A & \cos A & 0 \\ -\cos A & \sin A & 0 \\ 0 & 0 & 1 \end{bmatrix} \quad (A-1)$$

The pitch transformation is then a rotation through an angle P about the Y axis in the positive direction

$$P = \begin{bmatrix} \cos P & 0 & -\sin P \\ 0 & 1 & 0 \\ \sin P & 0 & \cos P \end{bmatrix} \quad (A-2)$$

Finally, the roll transformation is a rotation about the X axis in the positive direction,

$$R = \begin{bmatrix} 1 & 0 & 0 \\ 0 & \cos \Omega & \sin \Omega \\ 0 & -\sin \Omega & \cos \Omega \end{bmatrix} \quad (A-3)$$

The transformation from ENV coordinates to local ship coordinates is then accomplished by the product of these transformations, RPT. Conversely, the inverse transformation is accomplished by the transpose of these rotations, or

$$X_{ENV} = (RPT)^T X_{local}$$

In our case,  $X_{local}$  is  $X_0$ , the radar coordinates.

The transformation to ECF (earth-centered fixed) coordinates is made through the relations

$$\begin{aligned} X_{ECF} &= (RX) (TX + X_{ENV}) \\ &= (RX) [TX + (RPF)^T X_0] \end{aligned} \tag{A-4}$$

These coordinates are, of course, a function of time because  $\phi$  and  $\lambda$  are functions of time. RX and TX are given by the equations:

$$TX = \begin{bmatrix} 0 \\ -a_e e^2 \sin\phi \cos\phi / \sqrt{1-e^2 \sin^2\phi} \\ a_e \sqrt{1-e^2 \sin^2\phi} + H \end{bmatrix} \tag{A-5}$$

$$RX = \begin{bmatrix} -\sin\lambda & -\sin\phi \cos\lambda & \cos\phi \cos\lambda \\ \cos\lambda & -\sin\phi \sin\lambda & \cos\phi \sin\lambda \\ 0 & \cos\phi & \sin\phi \end{bmatrix} \tag{A-6}$$

where

$a_e$  = semi-major axis of the earth

$e$  = eccentricity of the earth

$\phi$  = geodetic latitude

$\lambda$  = geodetic longitude

It seems reasonable to assume that the change in  $\phi$  and  $\lambda$  from their values at some epoch time is independent of the initial values of  $\phi$  and  $\lambda$ . That is, let

$$\begin{aligned}\phi &= \phi_0 + \Delta\phi \\ \lambda &= \lambda_0 + \Delta\lambda\end{aligned}\tag{A-7}$$

with  $\Delta\phi$  and  $\Delta\lambda$  independent of  $\phi_0$  and  $\lambda_0$ .

Also, we would assume

$$H = H_0\tag{A-8}$$

since we hardly have any other choice using SINS data.

For program implementation, however, it is most convenient to assume that  $\Delta\phi$  and  $\Delta\lambda$  are equivalent to a change in earth centered fixed coordinates, which is independent of  $\phi_0$  and  $\lambda_0$ . This is the initial assumption which should be made. It requires that there be associated with each data point a change in earth centered coordinates for the radar. These coordinates may be placed on the data cards as follows:

	<u>Columns</u>	<u>Format</u>	<u>Units</u>
$\Delta\phi$	55 - 63	F9.7	radians
$\Delta\lambda$	64 - 72	F9.7	radians
$\Delta H$	73 - 80	F8.3	meters

APPENDIX B  
PROPAGATION OF ERRORS IN AN INERTIALLY GUIDED  
SURFACE VEHICLE WITH APPLICATION TO TRACKING  
SHIP ERROR REDUCTION

SECTION 1.0  
DERIVATION OF SINS ERROR EQUATIONS

1.1 INTRODUCTION

In this section, the equations of error propagation are developed for a local level inertial navigator. The equations are then simplified and the growth of error is obtained for the linearized case. The use of vehicle trajectory to reduce error growth is presented by comparing the errors obtained for rectilinear versus circular motion.

1.2 FUNDAMENTAL ERROR ANALYSIS EQUATIONS  
FOR SURFACE INERTIAL NAVIGATION SYSTEMS

The following set of equations defines the linearized dynamics of inertial navigator errors in terms of ground-speed velocity and position vectors. The space fixed results can be obtained by setting the angular rate vectors,  $\bar{\Omega}$  and  $\bar{\rho}$  to zero.

$$\dot{\bar{\psi}} = \bar{\psi} \times (\bar{\Omega} + \bar{\rho}) + \bar{\epsilon} \quad (1)$$

$$\epsilon \dot{\bar{V}}_g = \epsilon \bar{a} - (2\bar{\Omega} + \bar{\rho}) \times \epsilon \bar{V}_g + \epsilon \bar{g} \quad (2)$$

$$\epsilon \dot{\bar{R}} = \epsilon \bar{V}_g - \bar{\rho} \times \epsilon \bar{R} \quad (3)$$

$\bar{\psi}$  - a vector representing the infinitesimal rotation from computer to platform axes

$\bar{\Omega}$  - earth rate vector

$\bar{\rho}$  - commanded platform torquing relative to earth fixed basis

$\epsilon \bar{V}_g$  - Ground-speed error in earth fixed base

$\epsilon \bar{a}$  - vector made up of sources of acceleration measurement error

$\bar{\epsilon}_g$  - acceleration error vector caused by error  
in computing  $\bar{g}$

$\bar{R}$  - position vector in ideal platform base

$\bar{\epsilon}$  - drift rate of platform relative to computer  
axes.

Equation (1) shows the total drift rate is due to applying the total torquing rate  $(\bar{\Omega} + \bar{\rho})$  about misaligned axes plus the contribution of gyro drift. The acceleration equation and velocity equation are obtained by straightforward perturbation of the vector equations for ground speed and acceleration.

Note that the above equation is written in terms of the ideal platform analysis which are rotating in inertial space at a rate of  $(\bar{\Omega} + \bar{\rho})$ .

The acceleration measurement vector can be further broken down into the following components.

$$\bar{\epsilon}\bar{a} = \bar{b} + [K] \bar{A}_T + A_T \times \bar{\psi}$$

where

$\bar{b}$  is the vector of bias terms

$[K]$  is the diagonal scale factor error matrix

$\bar{A}_T$  is measured acceleration.

Similarly  $\bar{\epsilon}$  can be defined as:

$$\bar{\epsilon} = \dot{\phi}_0 + \dot{\phi}_{iA} + \dot{\phi}_{SA} + \dot{\phi}_{AN} + [C] (\bar{\Omega} + \bar{\rho})$$

Residual Drift

$$\dot{\phi}_0$$

This drift represents the uncertainty in the stray gyro torques which can not be calibrated out.

Mass Unbalance Drift

$$\dot{\phi}_{iA} \quad \dot{\phi}_{SA}$$

A mass unbalance about the output axis will produce a torque proportional to the accelerations along the input and spin axes. The terms  $\dot{\phi}_{iA}$  and  $\dot{\phi}_{SA}$  refer to drifts caused by mass unbalance along the input axis and spin axis respectively.

Anisoelastic Drift

$$\dot{\phi}_{AN}$$

This gyro drift is produced by the unequal deflection of the float and is proportional to the product of accelerations along the spin and input axes.

Scale Factor Error

$$[C]$$

The uncertainty in the gyro torquing scale factor produces this error for gyros that are torqued during navigation.  $[C]$  is assumed diagonal.

The most direct method of handling this system of linear equations is through the use of the state transition matrix concept. The state transition matrix approach simplifies the necessary computational bookkeeping and presents the equations in a form favorable to accurate integration by digital computer methods. A few mathematical preliminaries are in order:

$$\dot{\bar{X}} = [A] \bar{X} \quad (\text{Equations of State}) \quad (4)$$

$$[\dot{\phi}] = [A] [\phi] \quad (5)$$

$$\bar{X}(t) = [\phi(t, t_0)] \bar{X}(t_0) \quad (6)$$

where equation (4) represents vector shorthand for equations (1) through (3) and  $[\phi]$  is the state transition matrix. Note that  $[A]$  may be time varying. Equation (6) represents the response of the homogeneous equation stated in (4) to initial conditions. An appropriate example of the state transition matrix approach to inertial navigation error analysis is presented in the following formulation of the equations of state for a local level inertial navigator. The equations given utilize the following assumptions:

- Gyro and accelerometer axes are coincident with each other and are orthogonal in a local level mechanization.
- Errors caused by instrument misalignment and gyro anisoelasticity are negligible.

- The instrument axes are coincident with the ideal local level navigation axes.

None of these assumptions are particularly restrictive and could easily be waived at the expense of a more complicated set of equations.

EQUATIONS OF STATE FOR LOCAL LEVEL NAVIGATOR ERROR MODEL

$$\begin{bmatrix} \dot{x} \\ \dot{y} \\ \dot{z} \\ -\dot{x} \\ -\dot{y} \\ -\dot{z} \\ \dot{\psi}_x \\ \dot{\psi}_y \\ \dot{\psi}_z \\ \dot{\phi}_{xo} \\ \dot{\phi}_{xia} \\ \dot{\phi}_{xsa} \\ \dot{\phi}_{yo} \\ \dot{\phi}_{yia} \\ \dot{\phi}_{ysa} \\ \dot{\phi}_{zo} \\ \dot{\phi}_{zia} \\ \dot{\phi}_{zsa} \\ C_x \\ C_y \\ C_z \\ \delta_x \\ \delta_y \\ \delta_z \\ \delta'_x \\ \delta'_y \\ \delta'_z \\ \delta''_x \\ \delta''_y \\ \delta''_z \end{bmatrix} = \begin{bmatrix} \begin{bmatrix} 0 & \rho_z & -\rho_y \\ -\rho_z & 0 & \rho_x \\ \rho_y & -\rho_x & 0 \end{bmatrix} & \begin{bmatrix} I \\ 0 \end{bmatrix} \\ \begin{bmatrix} G & \begin{bmatrix} 0 & W_z & -W_y \\ -W_z & 0 & W_x \\ W_y & -W_x & 0 \end{bmatrix} & \begin{bmatrix} 0 & -A_z & A_y \\ A_z & 0 & -A_x \\ -A_y & A_x & 0 \end{bmatrix} & \begin{bmatrix} 0 \\ 0 \\ 0 \end{bmatrix} & \begin{bmatrix} 0 \\ 0 \\ 0 \end{bmatrix} & \begin{bmatrix} I \\ 0 \\ 0 \end{bmatrix} & \begin{bmatrix} A_x \\ A_y \\ A_z \end{bmatrix} \\ \begin{bmatrix} 0 \\ 0 \\ 0 \end{bmatrix} & \begin{bmatrix} 0 & W_z & -W_y \\ -W_z & 0 & W_x \\ W_y & -W_x & 0 \end{bmatrix} & \begin{bmatrix} 1 & A_y & A_z & 0 & 0 \\ 0 & 1 & A_z & A_x & 0 \\ 0 & 0 & 1 & A_x & A_y \end{bmatrix} & \begin{bmatrix} W_x & 0 & 0 \\ 0 & W_y & 0 \\ 0 & 0 & W_z \end{bmatrix} & \begin{bmatrix} 0 \\ 0 \\ 0 \end{bmatrix} \\ \begin{bmatrix} 0 \\ 0 \\ 0 \end{bmatrix} & \begin{bmatrix} 0 \\ 0 \\ 0 \end{bmatrix} \end{bmatrix}$$

where

$$W = \bar{\omega} + \bar{\rho}$$

Figure B-1

The last 18 equations represent the mathematical formalism for constant sources of error. Alternatively, if we view the error sources from a stochastic viewpoint, the variance of this set of variables is fixed with respect to time.

[ I ] represents an identity matrix of  
nxm order nxm

[ 0 ] represents a null matrix of dimension  
nxm nxm

[ G ] is the matrix of gravity partial  
differentials.

The X, Y and Z components given in the matrix equation refer to the two level coordinates which are arbitrarily oriented and the Z axis which is directed along the geodetic zenith (local vertical).

### 1.3 IMPLEMENTATION OF THE GENERAL SOLUTION FOR PROPAGATION OF ERROR

- Propagation of Error

The matrix equation given in (5) can be utilized directly in the solution for  $[\phi(t, t_0)]$ , where  $[\phi(t_0, t_0)] = [I]$ , each element of the  $\phi$  matrix representing the response of one state variable to a single initial condition. The data required for solution are:

- Profiles of the nominal trajectory, thrust acceleration, velocity and position.
- Estimates (covariance matrix) of the initial position, velocity and tilt errors as well as the gyro and accelerometer coefficients.

The former could be obtained from either a scientific simulation of the trajectory or from real data taken in an operational environment. The latter set of variables are dependent upon the uncertainty of calibration alignment and fix taking as well as statistical measurements of instrument performance.

If these data are available the state transition matrix is integrated using the trajectory forcing functions, computed from acceleration position and angular rate. The estimated values of the error variables are formulated as a covariance matrix having diagonal form if the random variables of the system are independent or if the interdependence is unknown. The covariance matrix of the error is then projected forward in time by the relation:

$$[C_{ov}(X(t), X(t))] = [\phi] [C_{ov}(X(o), X(o))] [\phi]^T$$

In addition, one may use the  $[\phi]$  to propagate deterministic errors forward in time in the form given in equation (6).

- Vertical Channel Stabilization

As given in the preceding matrix definitions, the navigation error equations are incomplete. In their present form, the error equations for vertical are inherently unstable, the vertical channel first order perturbation dynamics having the form of  $(S^2 - 2g_0/R_0)$  where  $S$  is the Laplace Operator variable. Therefore, all local level inertial navigation sets have an auxiliary sensor and equations to stabilize the vertical velocity and position. Normally, this consists of a barometric or radiometric altimeter.

The external data is mixed with the inertial data in the form of a linear filter network, the coefficients of which are chosen to reduce the error bounds to optimum limits. Typically, such an equation would have the form:

$$\begin{aligned} \bar{V}_z &= a_1(\bar{R}_z - \hat{R}_z) + \int \bar{W}_x \bar{W}_x \bar{R} dt \\ &+ \iint A_z dt + \int G(\hat{R}_z) dt \\ &+ a_2 \int (\bar{R}_z - \hat{R}_z) dt \end{aligned}$$

where

$\hat{R}_z$  - is the sum of externally derived altitude  
and the earth's radius vector

$\bar{R}_z$  - compensated value of position component  
in vertical direction

$\bar{V}_z$  - derivative of  $\bar{R}$  with respect to ideal  
platform basis

$a_1, a_2$  - constant coefficients of compensation  
loop

$G(\hat{R}_z)$  - gravitational acceleration computed  
from external measurements of altitude.

#### 1.4 SIMPLIFICATION OF THE ERROR EQUATIONS

If we consider a simplified model of the errors due to gravity;

$$G_x = g_0/R, \quad \epsilon g_x = G_x \cdot \epsilon \bar{R}_x$$

$$G_y = g_0/R, \quad \epsilon g_x = G_y \cdot \epsilon R_y$$

$$G_z = -2g_0/R, \quad \epsilon g_x = G_z \cdot \epsilon R_z$$

which neglects all terms of order greater than one. Differentiating (3) with respect to the ideal frame we have, after substituting for  $\epsilon \bar{V}_g$  and  $\epsilon V_g$

$$\begin{aligned} \epsilon \ddot{\bar{R}} + 2\bar{W} \times \epsilon \dot{\bar{R}} + \bar{\rho} \times \epsilon \bar{R} + [(\bar{W} + \bar{\Omega}) \cdot \epsilon \bar{R}] \bar{\rho} \\ + (\Omega^2 - W^2) \epsilon \bar{R} + [G] \epsilon \bar{R} = \epsilon \bar{a}. \end{aligned}$$

If we assume that  $\epsilon R_z$  and  $\epsilon \dot{R}_z$  are perfectly controlled by the external device previously discussed and substituting  $W_s^2 = g/R$  (Schuler frequency) we have for the horizontal channel errors:

$$\begin{aligned} \epsilon \ddot{R}_x + [(W_x + \Omega_x) \rho_x + W_s^2 + \Omega^2 - W^2] \epsilon R_x \\ - 2 W_z \epsilon \dot{R}_y + [(W_y + \Omega_y) \rho_x - \dot{\rho}_z] \epsilon R_y = \epsilon a_x \end{aligned} \quad (8)$$

$$\begin{aligned} \epsilon \ddot{R}_y + [(W_y + \Omega_y) \rho_y + W_s^2 + \Omega^2 - W^2] \epsilon R_y \\ - 2 W_z \epsilon \dot{R}_x + [(W_x + \Omega_x) \rho_y + \dot{\rho}_z] \epsilon R_x = \epsilon a_z \end{aligned} \quad (9)$$

since for all surface vessels,  $W_s^2$  is between one to two levels of magnitude greater than  $W^2$  and the coupling between the two axes can be seen to be rather weak since  $\rho$  and  $\dot{\rho}$  are quite small, the horizontal equation reduces to the following for the Free Azimuth ( $W_z = 0$ ) case:

$$\epsilon \ddot{R}_x + W_s^2 \epsilon R_x = b_x + K_x A_x + \psi_z A_y - \psi_y A_z \quad (8')$$

$$\epsilon \ddot{R}_y + W_s^2 \epsilon R_y = b_y + K_y A_y - \psi_z A_x + \psi_x A_z \quad (9')$$

In terms of Laplace Transforms, the above equations can be rearranged to show the "short term" (a few hours) error response to the most important input types.

• Response to Gyro Bias Error

$$\epsilon R_x(S) = \frac{\dot{\phi}_{z0}}{(S^2 + W_s^2) S} \cdot A_y(S) - \frac{\dot{\phi}_{y0} \cdot g}{(S^2 + W_s^2) S^2}$$

$$\epsilon R_y(S) = \frac{\dot{\phi}_{z0}}{(S^2 + W_s^2) S} \cdot A_x(S) + \frac{\dot{\phi}_{x0} \cdot g}{(S^2 + W_s^2) S}$$

where the cross coupling terms in equation (1) are considered negligible and  $A_z = |g|$ .  $A_x(S)$ ,  $A_y(S)$  are the La Place Transforms of the acceleration profiles.

• Response to Initial Tilt Error

$$\epsilon R_x(S) = \frac{\phi_{z0}}{S^2 + W_s^2} \cdot A_y(S) - \frac{\phi_{y0} \cdot g}{(S^2 + W_s^2) S}$$

$$\epsilon R_y(S) = \frac{\phi_{z0}}{S^2 + W_s^2} \cdot A_x(S) + \frac{\phi_{x0} \cdot g}{(S^2 + W_s^2) S}$$

- Response to Accelerometer Bias Error

$$\epsilon R_x = \frac{b_x}{S(S^2 + W_s^2)}$$

$$\epsilon R_y = \frac{b_y}{S(S^2 + W_s^2)}$$

- Response to Initial Velocity Error

$$\epsilon R_x = \frac{V_{ox}}{S^2 + W_s^2}$$

$$\epsilon R_y = \frac{V_{oy}}{S^2 + W_s^2}$$

- Gyro Scale Factor Error

Same form as gyro bias error except that  $\dot{\phi}_{z0}$  is replaced by  $C_z W_z$ ,  $\phi_{x0}$  is replaced by  $C_x W_x$  and  $\phi_{y0}$  is replaced by  $C_y W_y$ .

- Effect of Initial Heading Error

$$\epsilon R_x = V_y(s) \psi_{z0} / s$$

$$\epsilon R_y = V_x(s) \psi_{z0} / s$$

where

$$\psi_{z0} = \dot{\phi}_{z0}$$

1.5 CHOICE OF TRAJECTORY TO MINIMIZE ERROR PROPAGATION

The simplified equations obtained in the previous section show that for constant error sources and step acceleration, the error has the form of a sinusoid plus a constant, and is therefore, bounded for all errors except gyro drift error and gyro scale factor error. A brief table of position error for step input error sources is given below.

TABLE I  
ERROR PROPAGATION FOR  
STEP ACCELERATION

Error Source	Form of Error
Gyro Bias	$\epsilon R_{x,y} = K_{10} \left( t - \frac{1}{W_s} \sin W_s t \right)$
Gyro Scale Factor	$\epsilon R_{x,y} = K_{20} \left( t - \frac{1}{W_s} \sin W_s t \right)$
Accelerometer Bias	$\epsilon R_{x,y} = K_{30} (1 - \cos W_s t)$
Initial Tilt	$\epsilon R_{x,y} = K_{40} (1 - \cos W_s t)$
Velocity	$\epsilon R_{x,y} = K_{50} (1 - \cos W_s t)$
Heading	$\epsilon R_{x,y} = V_{y,x} \cdot \psi_{z0} \cdot t$

TABLE I (Cont.)

where

$$K_{10} = (\dot{\phi}_{z0} \cdot A_{y,x} \mp \dot{\phi}_{y,x0} \cdot g) / W_s^2$$

$$K_{20} = (C_{y,x} \cdot W_{y,y} \cdot (\mp g) + C_z W_z \cdot A_{y,x}) / W_s^2$$

$$K_{30} = b_{x,y} / W_s^2$$

$$K_{40} = \phi_{z0} A_{x,y} \mp \phi_{y,x0} \cdot g) / W_s^2 .$$

Note that the errors caused by gyro bias and heading error are not bounded in time and represent the worst class of errors. Consideration of the coupling terms in the  $\dot{\psi}$  equation which are ignored here, would worsen the situation since in the  $\bar{W}_{x,y} \times \bar{\psi}$  terms the first term is a function of velocity over the earth's surface. For the present, this effect will be lumped with unforced gyro drift.

It is clear, in any case, that the application of a constant acceleration step is to be avoided since the resultant error is unbounded. Therefore, trajectories other than straight line motion should be considered if vehicle motion is used to minimize system error.

• Circular Path Motion

If the vehicle follows a tight circular path at fairly low (surface ship) velocity, the acceleration profile can be given by

$$A_X(S) = \frac{AW_N}{S^2 + W_N^2} \quad ; \quad V_X = \frac{-(A/W_N)S}{S^2 + W_N^2}$$

$$A_Y(S) = \frac{A_S}{S^2 + W_N^2} \quad ; \quad V_Y = \frac{-A}{S^2 + W_N^2}$$

where the ship is assumed pointing at X at  $t_0$ , the acceleration magnitude is assumed constant and period of one cycle is  $\frac{2\pi}{W_N}$ . Applying this acceleration profile to the equations, we have the interesting results of Table II.

TABLE II  
ERROR PROPAGATION FOR  
SINUSOIDAL ACCELERATION

Gyro Bias

$$\epsilon R_X = K_{11} \left( \frac{1}{W_N} \sin W_N t - \frac{1}{W_S} \sin W_S t \right) + K_{12} \left( t - \frac{1}{W_S} \sin W_S t \right)$$

$$\epsilon R_y = K_{11} \left( \frac{W_N^2 - W_S^2}{W_S^2 W_N} - \frac{W_N}{W_S^2} \cos W_S t \right) + \frac{1}{W_N} \cos W_N t$$

$$+ K_{12} \left( t - \frac{1}{W_S} \sin W_S t \right)$$

Initial Tilt

$$\epsilon R_x = K_{41} (\cos W_N t - \cos W_S t)$$

$$+ K_{42} (1 - \cos W_S t)$$

$$\epsilon R_y = K_{41} \left( \sin W_N t - \frac{W_N}{W_S} \sin W_S t \right)$$

$$+ K_{42} (1 - \cos W_S t)$$

$$K_{11} = \frac{\dot{\phi}_{z0} A}{W_N^2 - W_S^2}$$

$$K_{12} = \bar{\tau} (\phi_{y0, x0} \cdot g) / W_S^2$$

$$K_{41} = \frac{\phi_{z0} A}{W_N^2 - W_S^2}$$

$$K_{42} = \bar{\tau} (\phi_{y0, x0} \cdot g) / W_S^2$$

## Initial Heading Error

$$\epsilon R_x = \frac{-A\psi_0}{W_N} (1 - \cos W_N t)$$

$$\epsilon R_y = A/W_N^2 \sin W_N t .$$

A substantial degree of improvement in the error growth is shown for the portion of these three terms which are contained in the general class of position errors induced by faulty heading reference. Clearly, a circular path is preferable to a rectilinear one when the location of the vessel become secondary to the reduction of error growth. Other trajectories could, for a given configuration, produce more optimum results but more information about the inertial navigator would be required before the more detailed computation required would be worthwhile.

SECTION 2.0  
SHORT PERIOD ERROR ANALYSIS OF A TRACKING SHIP  
INERTIAL NAVIGATOR FOR TWO TYPES OF MANEUVERS

2.1 INTRODUCTION

The error analysis equations for the decoupled, linearized horizontal channels of a local level inertial navigation set are utilized in this section to determine the following for two types of between pass maneuvers:

- Determination of the form of error growth for a velocity and position errors in each channel
- Computation of the error propagation produced by each error source for a given type of maneuver using "typical" magnitudes of error.
- Comparison of the relative merit of the cruise maneuvers.

The maneuvers referred to in the above describe the motion of the tracking ship during a two hour period between pass tracking intervals. The two classes of maneuvers considered are:

Case A - Constant Heading, Unaccelerated Motion

Case B - Circular Motion .

## ASSUMPTIONS AND APPROXIMATIONS

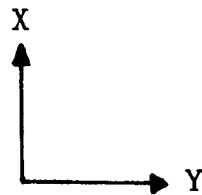
The linear uncoupled error equations for the horizontal channels of an inertial navigator are utilized throughout. The vertical channel error is assumed arbitrarily small and uncoupled with respect to the horizontal channels. The magnitudes for the error sources used in this report are of necessity, somewhat arbitrary, but represent reasonable estimates of the state-of-the-art instrument error budgets and "best guesses" for the initial velocity and platform tilt errors.

### Error Source Magnitudes

Gyro Bias	.03°/hr.
Accelerometer Bias	$1.0 \times 10^{-4}$ g
Initial Tilt	100 $\widehat{\text{sec}}$
Velocity	.2 Kts .

These errors are assumed independent and are the same magnitude for both channels. The effect of gyro torquer error and the error induced by torquing the misaligned platform axes is lumped in with the residual gyro bias term (.03°/hr.) Acceleration induced gyro drifts, accelerometer misalignments and all other sources of error are considered second order terms for the purpose of this study and are ignored in the analysis.

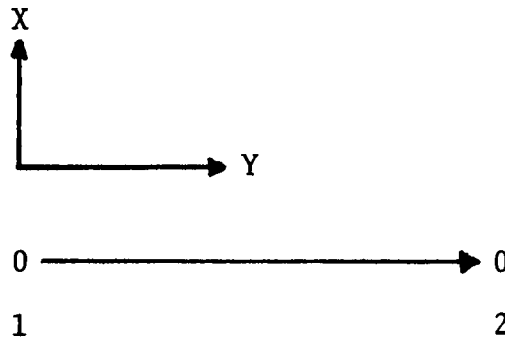
The instrument axes (gyro and accelerometer) are assumed to be orthogonal collinear, and nominally oriented along the computational X-Y axes direction shown below:



Case A - Unaccelerated Constant Heading

$V_{NON}$  - 10 Kts.

Heading - Positive Y Direction



Position ① represents initial position and ② is the nominal position of the vessel two hours later.

Error Source

Position Error

Gyro-Bias

$$\epsilon R_x = \frac{-\dot{\phi}_{y0} \cdot g}{W_s^2} \left( t - \frac{1}{W_s} \sin W_s t \right)$$

$$\epsilon R_y = \frac{\dot{\phi}_{x0} \cdot g}{W_s^2} \left( t - \frac{1}{W_s} \sin W_s t \right)$$

Heading Error

$$\epsilon R_x = V_0 \cdot \psi_{z0} \cdot t$$

$$\epsilon R_y = 0$$

Initial Tilt Error

$$\epsilon R_x = \frac{-\phi_{y0} \cdot g}{W_s^2} (1 - \cos W_s t)$$

$$\epsilon R_y = \frac{\phi_{x0} \cdot g}{W_s^2} (1 - \cos W_s t)$$

Accelerometer Bias Error

$$\epsilon R_x = \frac{b_x}{W_s^2} (1 - \cos W_s t)$$

$$\epsilon R_y = \frac{b_y}{W_s^2} (1 - \cos W_s t)$$

Initial Velocity Error

$$\epsilon R_x = \frac{\epsilon V_x}{W_s} \sin W_s t$$

$$\epsilon R_y = \frac{\epsilon V_y}{W_s} \sin W_s t$$

For Case A the form of error propagation is then

$$R_{x,y} = A \cdot t + B + C \sin (W_s t + \phi)$$

where the coefficients A,B,C and  $\phi$  depend on the manner in which the errors combine together. Note that only gyro bias and heading error contribute to the unbounded error. A plot of the magnitude of error for the X channel is given in Figure 1 for the assumed values of drift, bias and tilt given previously.

$$\begin{aligned}
V_o &= 10 \text{ Kts} \\
\dot{\phi}_{x_o, y_o} &= .03^\circ/\text{hr} \\
\phi_{x_o, y_o} &= 100 \widehat{\text{sec}} \\
\dot{\phi}_{z_o} &= \dot{\psi}_{z_o} = 100 \widehat{\text{sec}} \\
b_{x, y} &= 1.0 \times 10^{-4} \text{ g} \\
\epsilon V_{x, y} &= .2 \text{ Kts} .
\end{aligned}$$

The corresponding equations are given in Table B-1

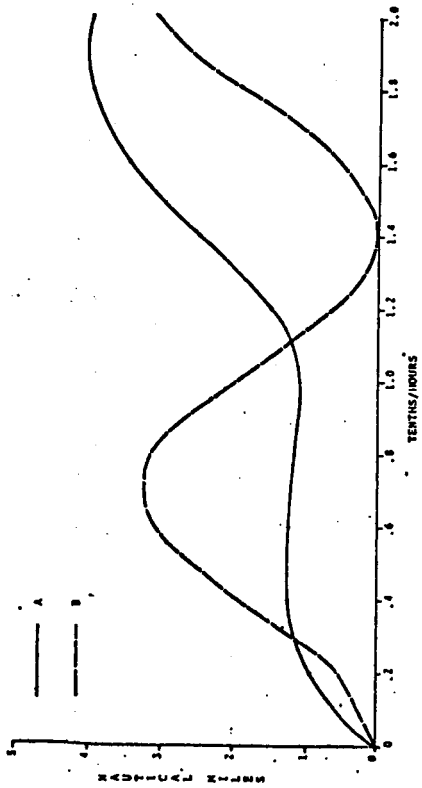
TABLE B-1  
X CHANNEL ERRORS FOR CASE A MANEUVERS

Gyro Bias Error	=	$1.83 (t + .41 \sin (4.46t))$
Heading Error	=	$4.84 \times 10^{-3} t$
Platform Tilt Error	=	$1.66 (1 - \cos (4.46t))$
Accelerometer Bias Error	=	$.344 (1 - \cos (4.46 t))$
Initial Velocity Error	=	$.0445 \sin (4.46t)$

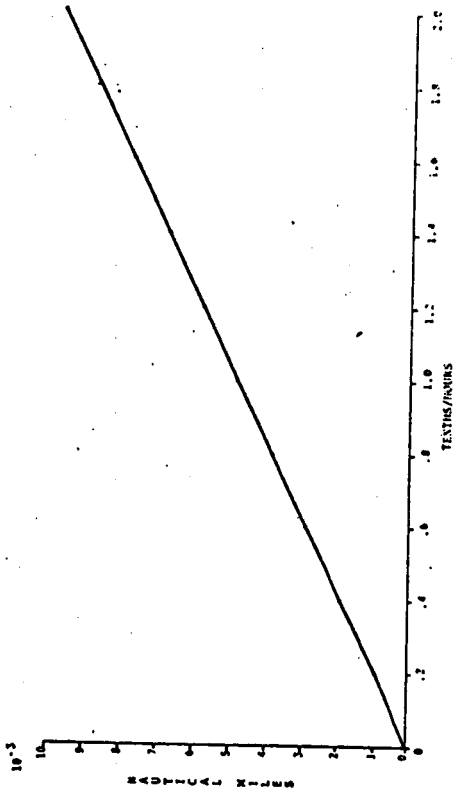
where the error above is expressed in nautical miles and t is given in hours.

FIGURE B-2

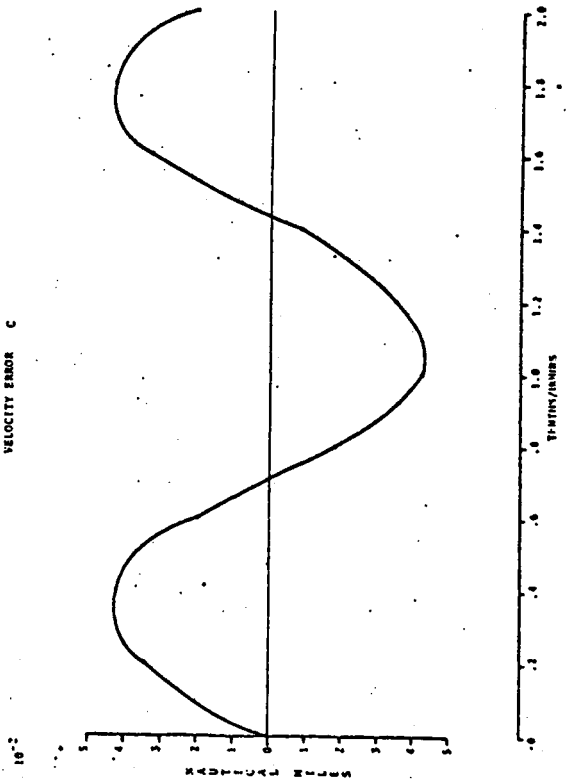
GYRO BIAS ERROR A  
PLATFORM TILT ERROR B



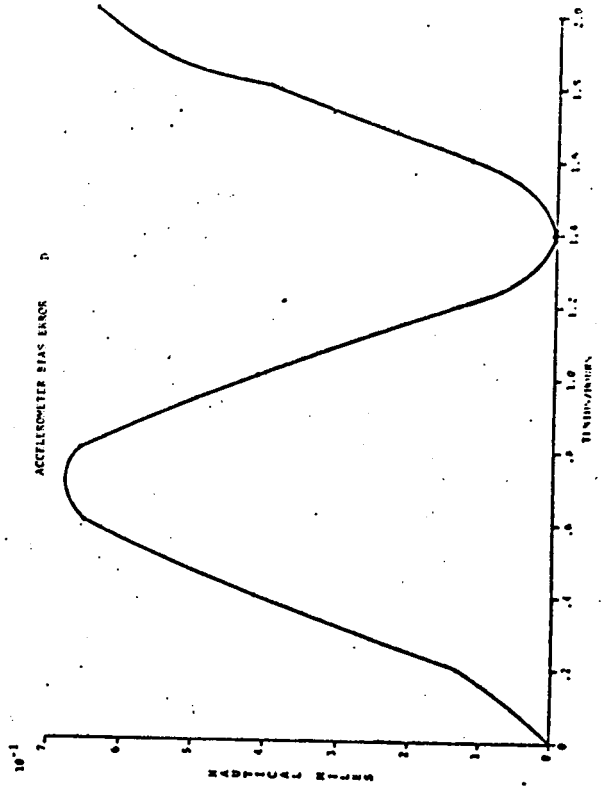
HEADING ERROR B



VELOCITY ERROR C



ACCELEROMETER BIAS ERROR D



Case B - Uniform Circular Motion

$$V_{\text{NOM}} = 10 \text{ Kts}$$

$$W_{\text{N}} = 2\pi / .334 \text{ rad/hr}$$

$$V_{\text{x}} = V_{\text{NOM}} \cos W_{\text{N}}t$$

$$V_{\text{y}} = V_{\text{NOM}} \sin W_{\text{N}}t$$

$$A_{\text{x}} = W_{\text{N}} V_{\text{NOM}} \sin W_{\text{N}}t$$

$$A_{\text{y}} = W_{\text{N}} V_{\text{NOM}} \cos W_{\text{N}}t .$$

It is apparent that the accelerometer bias and initial velocity errors are the same as for the previous case. The gyro bias and initial tilt contributions each have an additional term produced by the rotary acceleration and the heading error term is completely different.

Error SourcePosition Error

Gyro Bias

$$\frac{-\dot{\phi}_{x0} \cdot g}{W_s^2} \left( t - \frac{1}{W_s} \sin W_s t \right)$$

 $\epsilon R_x =$ 

$$+ \frac{W_N V_{NOM} \dot{\phi}_{z0}}{W_N^2 - W_s^2} \left( \frac{1}{W_N} \sin W_N t - \frac{1}{W_s} \sin W_s t \right)$$

$$\frac{\dot{\phi}_{x0} \cdot g}{W_s^2} \left( t - \frac{1}{W_s} \sin W_s t \right)$$

 $\epsilon R_y =$ 

$$- \frac{V_{NOM} \dot{\phi}_{z0}}{W_N^2 - W_s^2} \left[ \begin{array}{l} \frac{W_N^2 - W_s^2}{W_s^2 W_N} - \frac{W_N}{W_s} \cos W_s t \\ + \frac{1}{W_N} \cos W_N t \end{array} \right]$$

The additional terms produced by the circular motion and consequent acceleration are given in Table II with numerically evaluated coefficients for the given values of error terms and speed. A plot of these values over a two hour interval is given in Figure B-3. Most notably, the additional errors in gyro bias and platform tilt are very small in comparison to the gravity induced terms. The heading error is reduced by an order of magnitude for the circular motion case, but for the velocity and heading error magnitudes considered, this term is quite small.

Thus, unless the heading error magnitude is much greater than that utilized here. The growth of error is essentially the same for the two types of maneuvers considered.

If, however, a significant degree of unanticipated ship's acceleration occurs the circular maneuver would be superior since some cancelation of the effects of the pulses can be expected. For each acceleration impulse of magnitude A, the resultant additional error terms are:

$$\text{Gyro Bias} \quad \epsilon R''_{x,y} = \frac{\dot{\phi}_{z0} A_{y,x}}{W_s^2} (1 - \cos W_s t)$$

$$\text{Platform Tilt} \quad \epsilon R''_{x,y} = \frac{\phi_{z0} A_{y,x}}{W_s} \sin W_s t$$

Platform Tilt

$$\begin{aligned} & \frac{-\phi_{y0} \cdot g}{W_s^2} (1 - \cos W_s t) \\ \epsilon R_x = & \quad + \\ & \frac{+\phi_{z0} W_N V_{NOM}}{W_N^2 - W_s^2} \left[ \cos W_N t - \cos W_s t \right] \\ & \frac{\phi_{x0} \cdot g}{W_s^2} (1 - \cos W_s t) \\ \epsilon R_y = & \quad + \\ & \frac{-\phi_{x0} \cdot g}{W_N^2 - W_s^2} \left( \sin W_N t - \frac{W_N}{W_s} \sin W_s t \right) \end{aligned}$$

Heading Error

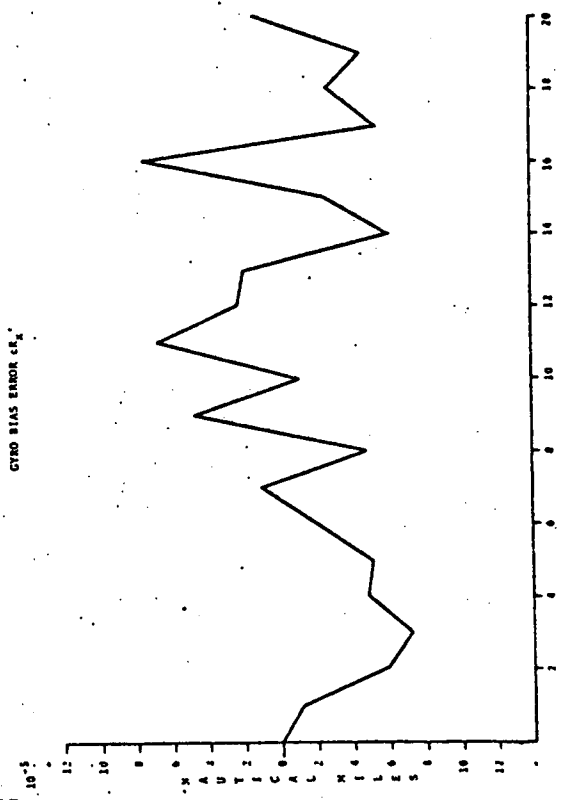
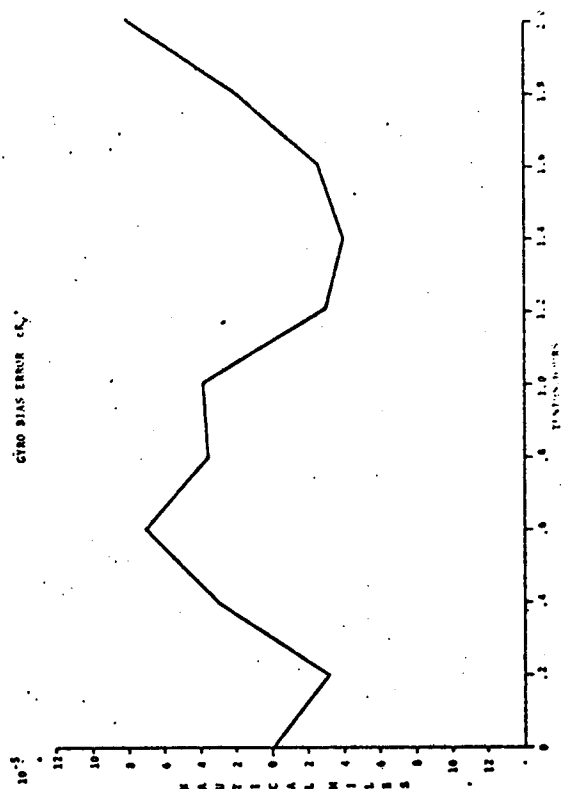
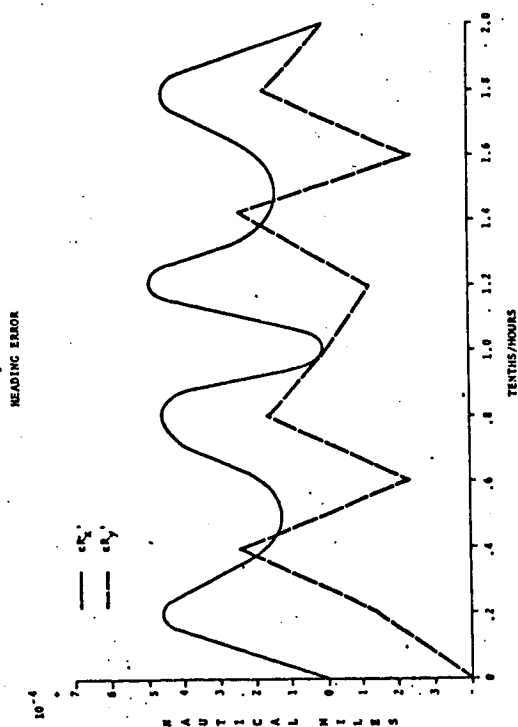
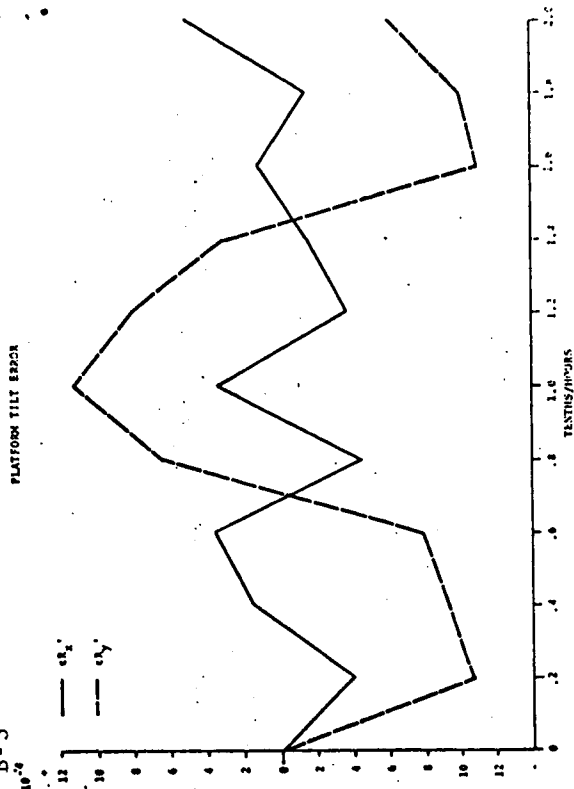
$$\begin{aligned} \epsilon R_x &= \frac{V_{NOM}}{W_N} \psi_{z0} (1 - \cos W_N t) \\ \epsilon R_y &= \frac{V_{NOM}}{W_N} \psi_{z0} \sin W_N t \end{aligned}$$

TABLE B-2  
 CIRCULAR MOTION INDUCED ERRORS  
 IN X AND Y CHANNELS

Gyro Bias Error	$\epsilon R'_x = 1.58 \times 10^{-5} \sin(18.8t) - 6.62 \times 10^{-5} \sin(4.46t)$ $\epsilon R'_y = 1.49 \times 10^{-5} \cos(4.46t) - 6.68 \times 10^{-5} + .84 \times 10^{-5} \cos(18.8t)$
Platform Tilt Error	$\epsilon R'_x = 2.73 \times 10^{-4} (\cos(18.8t) - \cos(4.46t))$ $\epsilon R'_y = 2.73 \times 10^{-4} (\sin(18.8t) - 4.42 \sin(4.46t))$
Heading Error	$\epsilon R'_x = 2.58 \times 10^{-4} (1 - \cos(18.8t))$ $\epsilon R'_y = 2.58 \times 10^{-4} \sin(18.8t)$

For  $\epsilon R'_{x,y}$  in Nautical Miles and t in Hours .

FIGURE B-3



SECTION 3.0  
SHORT PERIOD ERRORS FOR A  
DAMPED INERTIAL NAVIGATOR

3.1 INTRODUCTION

The damping of a marine inertial navigation system by means of an external source is generally accomplished by subtracting the reference velocity from the SINS velocity and adding the filtered difference to the measured acceleration as a correction. In terms of the short period error model, this amounts to providing negative feedback, i.e., damping for the error term at the expense of introducing a new error source. The filter used for the damping is considered a gain in the following which is consistent with the level of approximation implicit in the short term error model.

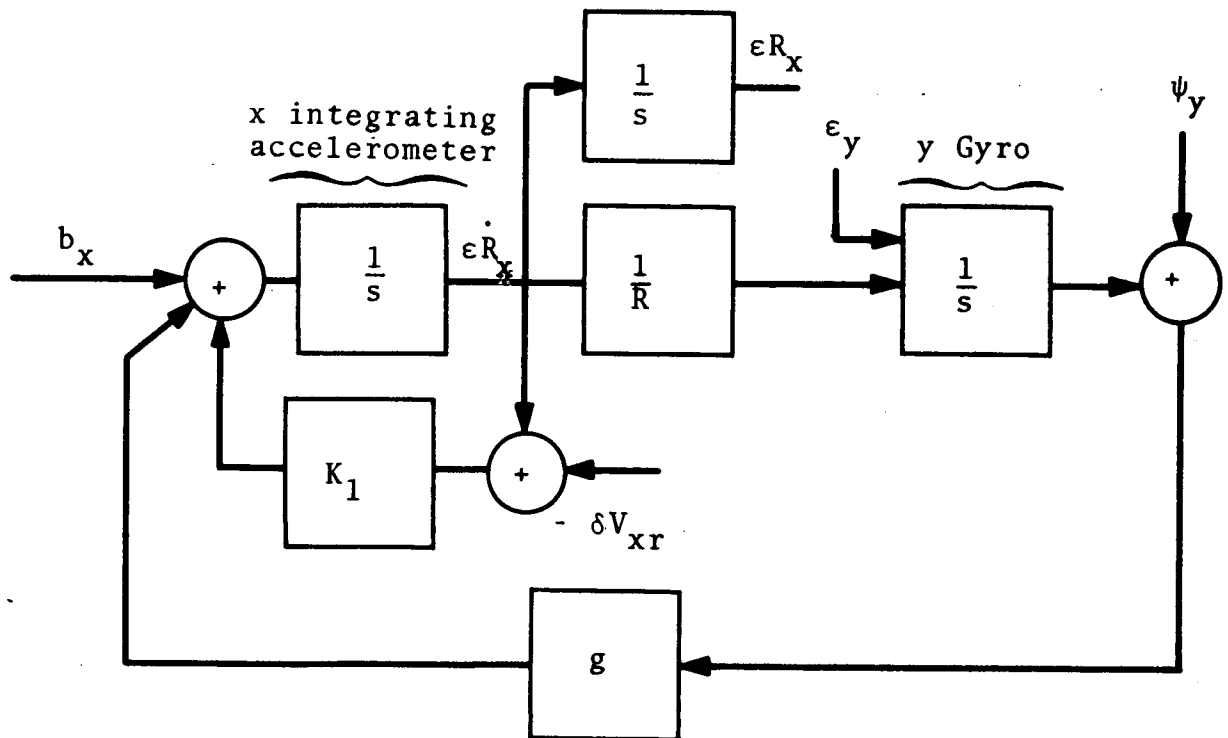
3.2 DAMPED INERTIAL NAVIGATOR ERROR EQUATIONS

$$\begin{aligned} \epsilon \ddot{R}_x + K_1 \epsilon \dot{R}_x + W_s^2 \epsilon R_x &= b_x + K_x A_x \\ &+ \psi_z A_y - \psi_y A_z \\ &+ K_1 \delta V_{xr} \end{aligned}$$

$$\begin{aligned} \epsilon \ddot{R}_y + K_1 \epsilon \dot{R}_y + W_s^2 \epsilon R_y &= b_y + K_y A_y \\ &- \psi_z A_y + \psi_x A_z \\ &+ K_1 \delta V_{yr} \end{aligned}$$

The short period errors produced by the damped system are shown in the following for the x channel in Figure B-4 and in the equations below based upon the following assumptions and approximations.

- 1) The vehicle is a slowly moving local level system, such that the horizontal (x,y) channels are uncoupled and independent.
- 2) For the time interval of interest the effect of the earth's rotation is negligible.



$b_x$ - bias error	$\epsilon \dot{R}_x$ - Velocity error
$\psi_y$ - platform tilt about y axis	$\epsilon R_x$ - Position error
$\epsilon_y$ - gyro drift about y axis	$K_1$ - Damping gain
$\delta V_{rx}$ - Velocity reference error in x direction	

FIGURE B-4: X CHANNEL ERROR MODEL

## X Channel Errors

- GYRO Drift

$$\epsilon R_x = -R \epsilon_y \begin{bmatrix} t - \frac{K_1}{W_s^2} + \frac{K_1}{W_s^2} e^{-(K_1/2)t} \cos(W_s' t) \\ - \left(1 - \frac{K_1^2}{2W_s^2}\right) / W_s' e^{-(K_1/2)t} \sin W_s' t \end{bmatrix}$$

- Platform Tilt

$$\epsilon R_x = R \psi_y \left(1 - e^{-(K_1/2)t} \left(\cos(W_s' t) + \frac{K_1}{2W_s'} \sin(W_s' t)\right)\right)$$

- Velocity Error

$$\frac{K_1 \delta V_{xr}}{W_s^2} \left(1 - e^{-(K_1/2)t} \left(\cos(W_s' t) + \frac{K_1}{2W_s} \sin(W_s' t)\right)\right) \cdot$$

• Accelerometer Bias

$$\frac{b_x}{W_s^2} \left( 1 - e^{- (K_1/2) t} \left( \cos (W_s' t) + \frac{K_1}{2W_s'} \sin (W_s' t) \right) \right)$$

where  $W_s$  - g/R Schuler frequency

$W_s'$  -  $(W_s^2 - \frac{K_1^2}{4})^{1/2}$  Reduced Schuler frequency

$\epsilon_y$  - Y gyro drift rate

$\psi_y$  - Platform tilt about Y axes

$\delta V_{xr}$  - Velocity reference error

$b_x$  - Accelerometer bias error

$t$  - time in hours .



These values are useful in determining the upper bounds of the error magnitudes permissible during the tracking period. For example, suppose the mission requires 100 meter accuracy during a two-hour tracking period and given that the system is perfectly quiescent at the initiation of tracking, we can determine the single source error bounds as follows:

Resultant Position  
Error After Two Hours

Permissible Single Error  
Source Magnitude

100 meters

GYRO Drift of .000385 °/hr.

or

Velocity Reference Error of .28 KNOTS

or

Platform tilt of 3  $\widehat{\text{sec}}$

or

Accelerometer Bias of  $1.67 \times 10^{-5}$  g.

In terms of error sources number two and three we are proscribing step changes in EM Log error or drift current of greater than .3 knots for the former and deflection of the local vertical step changes of more than 3 seconds of arc for the latter during the two-hour period. Since we have considered only one of two channels, the allowable error is even less than shown, however the magnitudes given are good "ball park numbers" and serve to illustrate that according to SINS specifications the ability of the unaided SINS to maintain 100 meters accuracy over a two-hour period is at best marginal.

### 3.4 AIDED INERTIAL OPERATION (SKOR)

The Sperry Kalman Optimal Reset (SKOR) program can be utilized during the tracking period in the STORE Mode to compute the best estimates of system errors obtained by performing a Kalman filtering operation utilizing the Marine Star Tracker (MST) measurements.

The output of the SKOR program is printed out at six minute intervals and should provide a considerable improvement over the unaided inertial system. However, the required usage of the MST is not possible if there is much cloud cover, in which case the system accuracy reverts back to that of the unaided SINS discussed previously.